Mathematical Biosciences and Engineering

http://www.aimspress.com/journal/MBE

MBE, 20(1): 402–436.
DOI: 10.3934/mbe.2023019
Received: 03 July 2022
Accepted: 25 September 2022
Revised: 22 September 2022
Published: 09 October 2022

Research article

New numerical dynamics of the fractional monkeypox virus model transmission pertaining to nonsingular kernels

Maysaa Al Qurashi[1,2], Saima Rashid[3,*], Ahmed M. Alshehri[4], Fahd Jarad[4,5,6,*] and Farhat Safdar[7]

[1] Department of Mathematics, King Saud University, P. O. Box 22452, Riyadh 11495, Saudi Arabia
[2] Department of Mathematics, Saudi Electronic University, Riyadh, Saudi Arabia
[3] Department of Mathematics, Government College University, Faisalabad 38000, Pakistan
[4] Department of Mathematics, King Abdulaziz University, Jeddah, Saudi Arabia
[5] Department of Mathematics, Cankaya University, Ankara, Turkey
[6] Department of Medical Research, China Medical University Hospital, China Medical University, Taichung, Taiwan
[7] Department of Mathematics, SBK for Women University, Quetta, Pakistan

* **Correspondence:** Email: saimarashid@gcuf.edu.pk, fahd@cankaya.edu.tr.

Abstract: Monkeypox (𝕄ℙ𝕏) is a zoonotic illness that is analogous to smallpox. Monkeypox infections have moved across the forests of Central Africa, where they were first discovered, to other parts of the world. It is transmitted by the monkeypox virus, which is a member of the Poxviridae species and belongs to the Orthopoxvirus genus. In this article, the monkeypox virus is investigated using a deterministic mathematical framework within the Atangana-Baleanu fractional derivative that depends on the generalized Mittag-Leffler (GML) kernel. The system's equilibrium conditions are investigated and examined for robustness. The global stability of the endemic equilibrium is addressed using Jacobian matrix techniques and the Routh-Hurwitz threshold. Furthermore, we also identify a criterion wherein the system's disease-free equilibrium is globally asymptotically stable. Also, we employ a new approach by combining the two-step Lagrange polynomial and the fundamental concept of fractional calculus. The numerical simulations for multiple fractional orders reveal that as the fractional order reduces from 1, the virus's transmission declines. The analysis results show that the proposed strategy is successful at reducing the number of occurrences in multiple groups. It is evident that the findings suggest that isolating affected people from the general community can assist in limiting the transmission of pathogens.

Keywords: Monkeypox virus model; Atangana-Baleanu differential operators; existence-uniqueness; qualitative analysis; Lagrangre interpolating polynomial

1. Introduction

Monkeypox (MPX) is a burgeoning contagious agent with a gradually increasing recurrence incidence and predicted breakout magnitude in human groups [1]. Inflammation, swollen glands and a dermatitis that produces blisters and then scabs over are among the symptoms (Figure 1). From the period of testing to the beginning of complications, it might take anywhere from 5 to 21 days. Symptoms last about 2 to 4 weeks on average. MPX infections have travelled beyond the woodlands of Central Africa, where they were first discovered, to various regions of the globe, where they are being transported. This mechanism of propagation is most probably connected to a global reduction in orthopoxvirus susceptibility following the termination of smallpox vaccination after the disease was declared eliminated in 1980. As a result, MPX could become the least common orthopoxvirus epidemic in human history [2]. The outbreak capability of MPX will tend to increase in a community exhibiting falling protective immunization versus orthopoxvirus organisms, according to mathematical techniques.

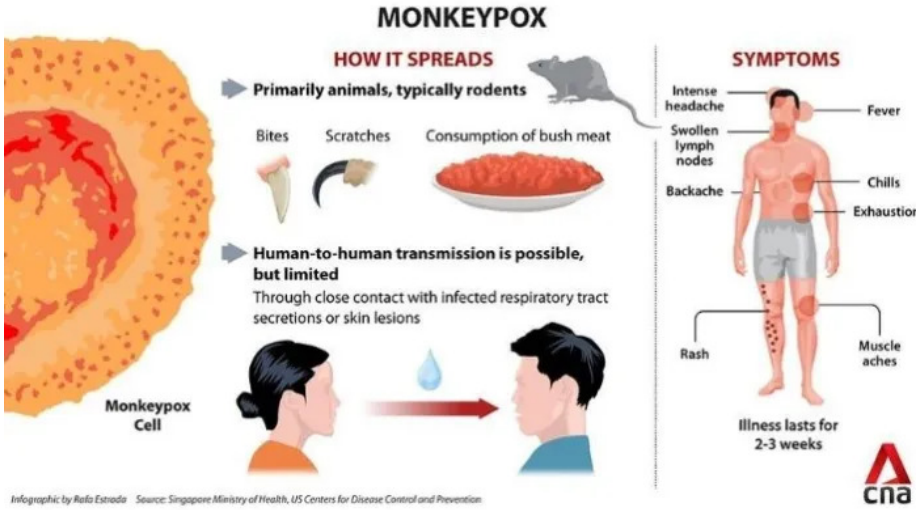

Figure 1. Transmission mechanism of MPX virus [3].

Furthermore, the MPX infection, a species of the orthopoxvirus genera in the Poxviridae category, causes MPX. The variola virus (which causes smallpox), chicken pox infection and adenovirus bacterial infection are all members of this family. Smallpox and MPX have common physiological manifestations, with MPX exhibiting lymphadenopathy slightly earlier in the illness phase as a differentiating characteristic [2]. Cowpox contamination results in long-lasting immunization; chickenpox recurrence incidence is only approximately 1 in 1000 over 15–20 years [4]. A first vaccine against cowpox with attenuated virus produces long-lasting resistance with an 80–95 % effectiveness. Prospective researchers have reported that prevention can persist for a considerable time. The present recommendation for amendment was introduced a decade ago [5]. Vaccinia has also been shown to provide long-lasting protection against MPX, with an effectiveness of 85 % [6].

Additionally, investigations of immunogenicity to orthopoxvirus genera imply that cowpox and MPX have excellent meld.

There have never been any reports of smallpox and MPX outbreaks occurring at the same time. Smallpox is a deadly pathogen, whereas MPX is a zoonotic virus that is highly contagious to humans via an unexplained arthropod vector. Interactions between mammalian genera in northern and southern African jungles, particularly in the northern African countries, the democratic states of the Congo, Cameroon, and Nigeria, culminate in intermittent MPX invasions into living creature species. All MPX breakouts have been self-contained, having living organism infection networks stop before outbreaks could develop [2]. MPX looks to be emerging as the most prevalent viral illness in people following the elimination of smallpox (Figure 2). People are generally understood to be at low danger of an outbreak [7].

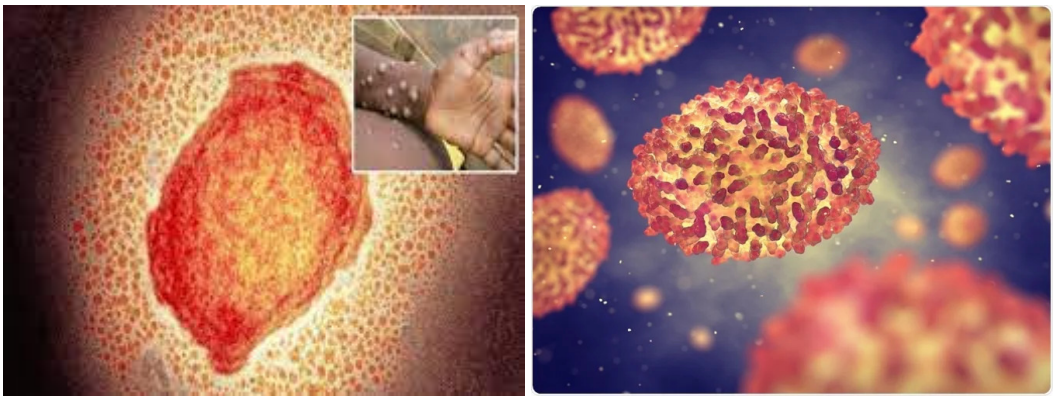

(a) (b)

Figure 2. (a) MPX virus particle, (b) MPX epidemiology [8].

Recently, MPX has come to be known as complex and requires a mammalian repository at this time since MPX human-to-human dissemination networks are comparatively limited; the greatest quantity of iterations described in research is seven [9]. However, as the H1N1 pandemic (swine flu) demonstrated, certain viral modifications can improve infectious viability in humans [10]. They have longitudinal, dual DNA chromosomes ranging from 130 to 230 kbp, and so they evolve at a far more moderate pace than H1N1. Despite this, they can adjust quickly [11], and genomic manipulation and contemporary molecular genetics have successfully transformed a mousepox infection into a particularly dangerous species [12].

To fully comprehend the unintended consequences of bacterial contamination and transmission, etiologic variational systems have been developed [13, 14]. The structure for a mathematical equation for MPX has been roughly established, but previous incarnations have experienced flaws in trying to acknowledge several of the virus's conditions associated with their completeness. Despite the fact that Bhunu and Mushayabasa [15] established a fundamental SIR vector-borne variational framework between humans and primates, they dismiss the possibility of an invasive condition in people. Usman and Adamu [16] extended this paradigm by integrating an SVEIR dimensional ability to estimate the virus's persistence duration and vaccination efficacy.

Fractional calculus adds dimensions to the explanation of complex phenomena in physical

processes involving memory impacts. However, researchers face significant challenges in defining such phenomena. This is because traditional fractional formulations have a unique kernel and therefore might not be equipped to adequately capture the non-locality of meaningful phenomena. Novel fractional derivatives featuring non-singular kernels have been proposed and implemented for pragmatic reasons in an attempt to accurately characterize nonlocal phenomena. The Mittag-Leffler (ML) [17] expressions are one of the leading contenders among known descriptions.

One of the most significant advantages of this novel derivative is that it exhibits innovative asymptotic behaviours that are distinct from those of fractional derivatives in their simplest rendition [18–21]. Furthermore, authentic mechanisms are being employed to investigate the properties of these adaptations, and appropriate numerical techniques should be refined to enable them to be accessible in application. To put it differently, the Atangana–Baleanu operator in the Caputo interpretation has an ML form kernel that permits it to preserve the Riemann–Liouville and Caputo derivatives for subsequent duration but just the Caputo–Fabrizio derivative for earlier generations [22–25]. The Atangana–Baleanu operator, more specifically, can encapsulate Brownian and unpredictable behavior, yielding crossover behavior. Careful analysis revealed that the Atangana–Baleanu operator can also represent strong predictive configurations, such as the multivariate Gaussian dispersion.

In new findings, it has been discovered that fractional-order formulations, in correlation with conventional ordinary formulae, have a stronger power to predict the non-local and unpredictable characteristics of diverse infections such as pneumonia-meningitis [26], diabetes [27], cholera [28], gastroenteritis [29], tuberculosis [30], hepatitis B virus [31], oncolytic virus [32], scabies [32] and several others [33–35]. Other scientific and mechanical frameworks [36–38] are advantageously adjusted in the domain of fractional derivatives because the discipline of fractional calculus includes the robust instruments of modeling a realistic world exhibiting significant memory consequences and irregularities [39–41].

The primary goal of this work was to analyze a novel fractional framework characterizing $\mathbb{MPX}$ and it was inspired by the preceding discussion and the work reported in [42, 43]. An extensive examination of the $\mathbb{MPX}$ model under fractional-order differential operators with the Atangana–Baleanu in the Caputo context was motivated by the flexibility of providing accessibility for clarity purposes. The Atangana-Baleanu fractional operator in the Caputo sense has been used to investigate the suggested system. An efficacious numerical approach proposed by the authors of [44] has been indeed adopted to handle these issues successfully. The following are the primary characteristics of the important milestones described in this article:

• The new technique just involves overcoming a simple recurrent mathematical expression for the proposed fractional operator. This research also includes an analysis of the indicated tool's existence-uniqueness that uses fixed point postulates. In comparison to other conventional systems, these features allow the suggested methodology to be inexpensive and simple to execute.

• The qualitative analysis of the $\mathbb{MPX}$ virus is discussed from a fractional standpoint.

• The stabilities of the disease-free and endemic equilibria are presented out in a detailed manner, taking into account the Routh-Hurwitz threshold.

• The modeling results show that emerging projections rely on a fractional operator and exhibit significantly more asymptomatic behavior than classical systems.

• The novel fractional form featuring ML kernels generates projections that are significantly correlated by using a handful of quantified evidence, according to numerical studies.
As a result, fractional calculus makes it possible to create increasingly comprehensive assessments of evolutionary phenomena, facilitating more revolutionary techniques of their complicated behaviours.

2. Model illustration

In this part, the Atangana-Baleanu-Caputo (ABC) fractional derivative form of the $\mathbb{MPX}$ epidemic mathematical systems is introduced. Let us just continue with a review of the ML kernels' notions and their concerning consequences.

Definition 2.1. *([17]) For $\rho \in [0,1]$, $\mathbf{c} < \mathbf{d}$ and $\mathcal{F}_1 \in H^1(\mathbf{c},\mathbf{d})$, the ABC derivative of fractional-order for $\mathcal{F}_1$ is presented as*

$$ {}^{ABC}\mathbf{D}^{\rho}\mathcal{F}_1(\tau) = \frac{\mathbb{ABC}(\rho)}{(1-\rho)}\int_{\mathbf{c}}^{\tau}\frac{d\mathcal{F}_1}{d\tau}E_{\rho}\Big(\frac{\rho}{\rho-1}(\tau-\varrho)^{\rho}\Big)d\varrho, \tag{2.1}$$

where $\mathbb{ABC}(\rho)$ is a normalization mapping satisfying $\mathbb{ABC}(0) = \mathbb{ABC}(1) = 1$ and the ML function signified by $E_\rho(z_1)$ having the set of complex numbers $\mathbb{C}$ is defined as

$$E_{\rho}(z_1) = \sum_{\gamma=0}^{\infty}\frac{z_1^{\gamma}}{\Gamma(\rho\gamma+1)},\ \ \rho, z_1 \in \mathbb{C},\ \ \Re(\rho) > 0.$$

Definition 2.2. *([17]) For $\rho \in [0,1]$, $\mathbf{c} < \mathbf{d}$ and $\mathcal{F}_1 \in H^1(\mathbf{c},\mathbf{d})$, the Atangana–Baleanu (AB) fractional integral of $\mathcal{F}_1$ is presented as*

$$ {}^{AB}_{\mathbf{c}}\mathbf{I}^{\rho}_{\tau}\mathcal{F}_1(\tau) = \frac{(1-\rho)}{\mathbb{ABC}(\rho)}\mathcal{F}_1(\tau) + \frac{\rho}{\Gamma(\rho)\mathbb{ABC}(\rho)}\int_{\mathbf{c}}^{\tau}\mathcal{F}_1(\varrho)(\tau-\varrho)^{\rho-1}d\varrho. \tag{2.2}$$

Lemma 2.1. *([42]) (Newton-Leibniz identity) For $\mathcal{F}_1 \in \mathbb{C}^1(\mathbf{c},\mathbf{d})$, the ABC fractional derivative and integral for $\mathcal{F}_1$ holds:*

$$ {}^{AB}_{\mathbf{c}}\mathbf{I}^{\rho}_{\tau}\big({}^{ABC}_{\mathbf{c}}\mathbf{D}^{\rho}_{\tau}\mathcal{F}_1(\tau)\big) = \mathcal{F}_1(\tau) - \mathcal{F}_1(\mathbf{c}). \tag{2.3}$$

Lemma 2.2. *([42]) For $\mathbf{c} < \mathbf{d}$, $\mathcal{F}_1, \mathcal{F}_2 \in H^1(\mathbf{c},\mathbf{d})$, the ABC fractional derivative holds for the subsequent variant:*

$$\Big\| {}^{ABC}_{\mathbf{c}}\mathbf{D}^{\rho}_{\tau}\mathcal{F}_1(\tau) - {}^{ABC}_{\mathbf{c}}\mathbf{D}^{\rho}_{\tau}\mathcal{F}_2(\tau)\Big\| \le H\Big\|\mathcal{F}_1(\tau) - \mathcal{F}_2(\tau)\Big\|. \tag{2.4}$$

Our next result is the generalized mean-value theorem, which is mainly due to [42].

Lemma 2.3. *([42]) Assume there is a function $h_1(\varrho) \in \mathbb{C}[\mathbf{c},\mathbf{d}]$ and also suppose ${}^{ABC}_{0}\mathbf{D}^{\rho}_{\tau}h_1(\varrho) \in \mathbb{C}[\mathbf{c}, q_2]$ and $\rho \in (0,1]$. Then $h_1(\varrho) = h_1(\mathbf{c}) + \frac{1}{\Gamma(\rho)}\,{}^{ABC}_{0}\mathbf{D}^{\rho}_{\tau}h_1(\chi)(\varrho-\mathbf{c})^{\rho}, \chi \in [0,\varrho]$.*

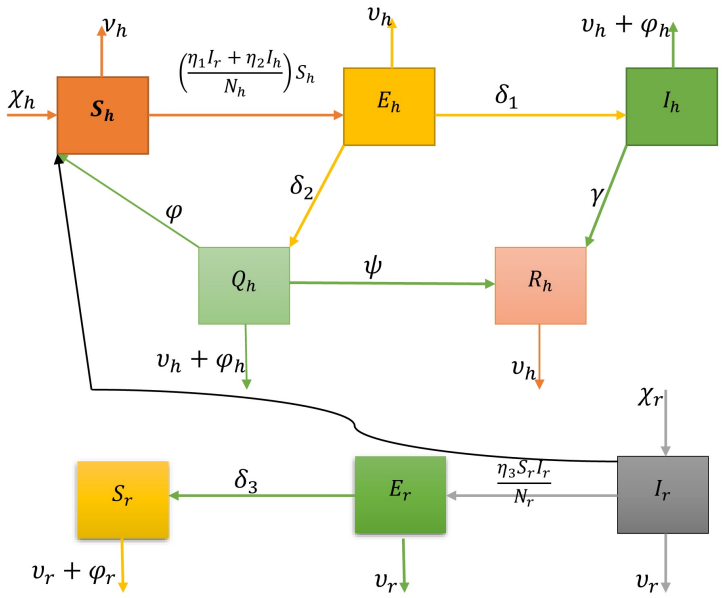

Figure 3. Schematic configuration of $\mathbb{MPX}$ virus.

Followed by Lemma 2.3, for $\rho \in (0, 1]$, if $h_1(\varrho) \in [0, \mathbf{d}]$, ${}_0^{ABC}\mathbf{D}_\tau^\rho h_1(\varrho) \in (0, \mathbf{d}]$ and ${}_0^{ABC}\mathbf{D}_\tau^\rho h_1(\varrho) \geq 0$ for all $\varrho \in (0, \mathbf{d}]$, then the mapping $h_1(\varrho)$ is increasing. Otherwise, $h_1(\varrho)$ is said to be decreasing for all $\varrho \in [0, \mathbf{d}]$.

We will now proceed to design the $\mathbb{MPX}$ model. The configuration diagram below (Figure 3) was utilized to construct the numerical structure for this analysis.

The explanatory features of the system are examined in this section. To streamline the approach, we divided the coherent model into several Differential equations (DEs), as shown in (2.5), that are estimations for ($\mathbb{MPX}$).

The underlying formulations, which are established on the basis of the process, describe the numerical technique involving the mathematical model implemented in this research.

$$\begin{cases} \dot{\mathbf{S}}_\hbar(\tau) = \chi_\hbar - \frac{(\eta_1 \mathbf{I_r} + \eta_2 \mathbf{I}_\hbar)\mathbf{S}_\hbar}{\mathbf{N}_\hbar} - \upsilon_\hbar \mathbf{S}_\hbar + \sigma \mathbf{Q}_\hbar, \\ \dot{\mathbf{E}}_\hbar(\tau) = \frac{(\eta_1 \mathbf{I_r} + \eta_2 \mathbf{I}_\hbar)\mathbf{S}_\hbar}{\mathbf{N}_\hbar} - (\delta_1 + \delta_2 + \upsilon_\hbar)\mathbf{E}_\hbar, \\ \dot{\mathbf{I}}_\hbar(\tau) = \delta_1 \mathbf{E}_\hbar - (\upsilon_\hbar + \varphi_\hbar + \gamma)\mathbf{I}_\hbar, \\ \dot{\mathbf{Q}}_\hbar(\tau) = \delta_2 \mathbf{E}_\hbar - (\sigma + \upsilon_\hbar + \varphi_\hbar + \psi)\mathbf{Q}_\hbar, \\ \dot{\mathbf{R}}_\hbar(\tau) = \gamma \mathbf{I}_\hbar + \psi \mathbf{Q}_\hbar - \upsilon_\hbar \mathbf{R}_\hbar, \\ \dot{\mathbf{S}}_\mathbf{r}(\tau) = \chi_\mathbf{r} - \frac{\eta_3 \mathbf{S_r} \mathbf{I_r}}{\mathbf{N_r}} - \upsilon_\mathbf{r} \mathbf{S_r}, \\ \dot{\mathbf{E}}_\mathbf{r}(\tau) = \frac{\eta_3 \mathbf{S_r} \mathbf{I_r}}{\mathbf{N_r}} - (\upsilon_\mathbf{r} + \delta_3)\mathbf{E_r}, \\ \dot{\mathbf{I}}_\mathbf{r}(\tau) = \delta_3 \mathbf{E_r} - (\upsilon_\mathbf{r} + \varphi_\mathbf{r})\mathbf{I_r}. \end{cases} \tag{2.5}$$

Here, we present a deterministic compartmental framework of $\mathbb{MPX}$ propagation and prevention, including two communities: individuals and rodents. Susceptible individuals $\mathbf{S}_\hbar(t_1)$, vulnerable individuals $\mathbf{E}_\hbar(t_1)$, infectious individuals $\mathbf{I}_\hbar(t_1)$, segregated individuals $\mathbf{Q}_\hbar(t_1)$ and human restoration

Table 1. Explanation of the attributed values assumed in the model.

Symbols	Explanations	Values	References
$\chi_{\hbar}$	Proportion of humans acquisition	0.029	[45]
$\chi_{\mathbf{r}}$	Proportion of rodents acquisition	0.2	[45]
η_1	Rodent-human interaction rate	0.00025	[46]
η_2	Rate of human-to-human interaction	0.00006	[46]
η_3	Rate of rodent-to-rodent interaction	0.027	[46]
δ_1	Rate of exposed people to infectious people	0.2	Supposed
δ_2	Rate of confirmed reported incidents	2.0	Estimated
σ	Rate of untreated after screening	2.0	Estimated
ψ	Transition from the separated to the restored group	0.52	Supposed
γ	Humans' rate of recuperation	0.83	[45]
$\upsilon_{\hbar}$	Natural mortality rate for people	1.5	[46]
$\upsilon_{\mathbf{r}}$	Natural mortality rate for rodents	0.002	[46]
$\varphi_{\hbar}$	Proportion of rodents dying as a result of disease	0.5	Supposed
$\varphi_{\mathbf{r}}$	Proportion of humans dying as a result of disease	0.2	[47]

$\mathbf{R}_{\hbar}(t_1)$ are the five categories of the global community. Susceptible rodents $\mathbf{S}_{\mathbf{r}}(t_1)$, revealed rodents $\mathbf{E}_{\mathbf{r}}(t_1)$ and infectious rodents $\mathbf{I}_{\mathbf{r}}(t_1)$ are the three categories of the rodent community. The proportion of enlistment into the global community is $\chi_{\hbar}$. η_1 is the component of the efficacious interaction yield and the possibility of a sentient contracting the pathogen after coming into contact with a contaminated rodent, and η_2 is the outcome of the impact correspondence yield and the plausibility of a sentient contracting the pathogen after coming into contact with a highly contagious person. The rate of reported cases who becoming extremely contaminated is δ_2, while the population of individuals of becoming diseased is δ_1. Several suspicious instances are validated after diagnostic testing, while the rest are not identified and are transferred to susceptibility populations at a pace σ. At an incidence of ψ, suspicious infections are diagnosed and shifted to the restored group. Adult recuperation capacity is increasing at a rate of γ. Spontaneous mortality happens at speeds of $\upsilon_{\hbar}$ and $\upsilon_{\mathbf{r}}$ in the adult and rodent populations, respectively. The appropriate connection incidence is based on η_3, which is the possibility of a rodent being contaminated per encounter with an infectious rodent. Both the spontaneous fatality rate $\upsilon_{\mathbf{r}}$ and the illness fatality rate $\varphi_{\mathbf{r}}$ reduced the diseased rodent community. The crossover between the several cohorts addressed in the system is depicted in Figure 3, and the system is controlled by the nonlinear differential equations listed below.

3. Qualitative aspects of ABC fractional $\mathbb{MPX}$ virus

3.1. Invariant region

First we find the invariant region, which confirms that the solution is bounded. Therefore, we assume the overall human population is $\mathbf{N}_{\hbar} = \mathbf{S}_{\hbar} + \mathbf{E}_{\hbar} + \mathbf{I}_{\hbar} + \mathbf{Q}_{\hbar} + \mathbf{R}_{\hbar}$ and the rodent population is $\mathbf{N}_{\mathbf{r}} = \mathbf{S}_{\mathbf{r}} + \mathbf{E}_{\mathbf{r}} + \mathbf{I}_{\mathbf{r}}$.

The fractional version of the biologically viable domain $\Phi = \Phi_{\hbar} \times \Phi_{\mathbf{r}}$ for the $\mathbb{MPX}$ virus system

(2.5), i.e., $\Phi_\hbar \subset \mathbf{R}^5_+$ and $\Phi_{\mathbf{r}} \subset \mathbf{R}^3_+$ is such that

$$\Phi_\hbar := \Big\{(\mathbf{S}_\hbar, \mathbf{E}_\hbar, \mathbf{I}_\hbar, \mathbf{Q}_\hbar, \mathbf{r}_\hbar) \in \mathbb{R}^5_+ : \mathbf{N}_\hbar \leq \frac{\chi_\hbar}{\upsilon_\hbar}\Big\}$$

and

$$\Phi_{\mathbf{r}} := \Big\{(\mathbf{S}_{\mathbf{r}}, \mathbf{E}_{\mathbf{r}}, \mathbf{I}_{\mathbf{r}}) \in \mathbb{R}^3_+ : \mathbf{N}_\hbar \leq \frac{\chi_{\mathbf{r}}}{\upsilon_{\mathbf{r}}}\Big\}.$$

Lemma 3.1. *If there is an* $\mathbb{MPX}$ *virus system* (2.5) *having initial conditions (ICs) in Domain* Φ *is positively invariant.*

Proof. Now, to illustrate the boundedness of the solutions of the $\mathbb{MPX}$ virus system (2.5), we proceed by accumulating all of the model's formulas, which yields

$$\begin{aligned} {}^{ABC}_{0}\mathbf{D}^{\rho}_{t_1}\mathbf{N}_\hbar(t_1) &= \chi_\hbar - \upsilon_\hbar \mathbf{S}_\hbar - \upsilon_\hbar \mathbf{E}_\hbar - (\upsilon_\hbar + \varphi_\hbar)\mathbf{I}_\hbar - (\upsilon_\hbar + \varphi_\hbar)\mathbf{Q}_\hbar - \upsilon_\hbar \mathbf{R}_\hbar \\ &= \chi_\hbar - \upsilon_\hbar \mathbf{N}_\hbar - \varphi_\hbar(\mathbf{I}_\hbar + \mathbf{Q}_\hbar) \\ &\leq \chi_\hbar - \upsilon_\hbar \mathbf{N}_\hbar. \end{aligned}$$

Implementing the Laplace transform, we find that

$$\mathcal{L}({}^{ABC}_{0}\mathbf{D}^{\rho}_{t_1}\mathbf{N}_\hbar(t_1) + \upsilon_\hbar \mathbf{N}_\hbar(t_1)) \leq \mathcal{L}(\chi_\hbar).$$

It follows that

$$\mathcal{L}(\mathbf{N}_\hbar) \leq \Big(1 - \frac{\ell_1 \rho}{(1-\ell_1)(1-\rho)} s_1^{-\rho}\Big)^{-1}\Big\{\frac{1-\rho}{(1-\ell_1)\mathbb{ABC}(\rho)}\Big(1 + \frac{\rho}{1-\rho}s_1^{-\rho}\Big)\frac{\chi_\hbar}{s_1} + \mathbf{N}_\hbar(0)\frac{1}{s_1(1-\ell_1)}\Big\},$$

where $\ell_1 = -\frac{\upsilon_\hbar(1-\rho)}{\mathbb{ABC}(\rho)}$.

By implementing the approach described in [35] and using the solution produced by employing the inverse Laplace transform, we have

$$\begin{aligned} \mathbf{N}_\hbar(t_1) &= \frac{\chi_\hbar}{\upsilon_\hbar} - \frac{\chi_\hbar}{\upsilon_\hbar(1-\ell_1)}\frac{d}{dt_1}\int_0^{t_1} E_\rho\Big(\frac{\ell_1\rho}{(1-\ell_1)(1-\rho)}(t_1 - x_1)^\rho\Big)dx_1 \\ &\quad + \frac{1}{1-\ell_1}E_\rho\Big(\frac{\ell_1\rho}{(1-\ell_1)(1-\rho)}(t_1)^\rho\Big)\mathbf{N}_\hbar(0). \end{aligned}$$

Repeating the analogous process for the rodent population, we have

$$\begin{aligned} \mathbf{N}_{\mathbf{r}}(t_1) &= \frac{\chi_\hbar}{\upsilon_{\mathbf{r}}} - \frac{\chi_{\mathbf{r}}}{\upsilon_{\mathbf{r}}(1-\ell_2)}\frac{d}{dt_1}\int_0^{t_1} E_\rho\Big(\frac{\ell_2\rho}{(1-\ell_2)(1-\rho)}(t_1 - x_1)^\rho\Big)dx_1 \\ &\quad + \frac{1}{1-\ell_2}E_\rho\Big(\frac{\ell_2\rho}{(1-\ell_2)(1-\rho)}(t_1)^\rho\Big)\mathbf{N}_{\mathbf{r}}(0), \end{aligned}$$

where $\ell_2 = -\frac{\upsilon_{\mathbf{r}}(1-\rho)}{\mathbb{ABC}(\rho)}$.

Here, in both cases the ML function is denoted by E_{ν_1,ν_2}. Based on the assumption that the ML function possesses asymptotic tendency, we have

$$E_{\nu_1,\nu_2} \approx \sum_{k=1}^{w} z_1^{-k}/\Gamma(\nu_2 - \nu k) + O(1/|z_1|^{1+w}), \;\; |z_1| \mapsto \infty, \; \nu_1\pi/2 < |Arg(z_1)| \leq \pi.$$

Consequently, $\mathbf{N}_\hbar(t_1)$ and $\mathbf{N}_\mathbf{r}(t_1)$ converges for $t_1 \mapsto \infty$. Hence, the domain Φ is positively invariant.

Now, we demonstrated the accompanying result by applying a (Lemma 2.3 from [42]) and the fractional comparative criterion [48].

Assume that there is a solution $(\mathbf{S}_\hbar, \mathbf{E}_\hbar, \mathbf{I}_\hbar, \mathbf{Q}_\hbar, \mathbf{R}_\hbar, \mathbf{S}_\mathbf{r}, \mathbf{E}_\mathbf{r}, \mathbf{I}_\mathbf{r})$ involved in the ICs of $\mathbb{R}^5_+ \times \mathbb{R}^3_+$. Then, the $\mathbb{R}^5_+ \times \mathbb{R}^3_+$ domain is a positively invariant set of the system (2.5).

Based on the scheme described in [49], we intended to define the existence-uniqueness of the $\mathbb{MPX}$ virus dynamics (2.5); thus, we have

$$\begin{cases} {}^{ABC}\mathbf{D}^{\rho}_{t_1}\mathbf{S}_\hbar(\tau)\big|_{\mathbf{S}_\hbar=0} = \chi_\hbar \geq 0, \\ {}^{ABC}\mathbf{D}^{\rho}_{t_1}\mathbf{E}_\hbar(\tau)\big|_{\mathbf{E}_\hbar=0} = 0, \\ {}^{ABC}\mathbf{D}^{\rho}_{t_1}\mathbf{I}_\hbar(\tau)\big|_{\mathbf{I}_\hbar=0} = \delta_1\mathbf{E}_\hbar \geq 0, \\ {}^{ABC}\mathbf{D}^{\rho}_{t_1}\mathbf{Q}_\hbar(\tau)\big|_{\mathbf{Q}_\hbar=0} = \delta_2\mathbf{E}_\hbar \geq 0, \\ {}^{ABC}\mathbf{D}^{\rho}_{t_1}\mathbf{R}_\hbar(\tau)\big|_{\mathbf{R}_\hbar=0} = \gamma\mathbf{I}_\hbar + \psi\mathbf{Q}_\hbar \geq 0, \\ {}^{ABC}\mathbf{D}^{\rho}_{t_1}\mathbf{S}_\mathbf{r}(\tau)\big|_{\mathbf{S}_\mathbf{r}=0} = \chi_\mathbf{r} \geq 0, \\ {}^{ABC}\mathbf{D}^{\rho}_{t_1}\mathbf{E}_\mathbf{r}(\tau)\big|_{\mathbf{E}_\mathbf{r}=0} = 0, \\ {}^{ABC}\mathbf{D}^{\rho}_{t_1}\mathbf{I}_\mathbf{r}(\tau)\big|_{\mathbf{I}_\mathbf{r}=0} = \delta_3\mathbf{E}_\mathbf{r} \geq 0. \end{cases} \tag{3.1}$$

Observe that (3.1) shows that every solution of (2.5) is nonnegative and remains in Φ; we have that

$$0 \leq \mathbf{N}_\hbar(t_1) \leq \mathbf{N}_\hbar(0)\exp(-\upsilon_\hbar t_1) + \frac{\chi_\hbar}{\upsilon_\hbar}(1 - \exp(-\upsilon_\hbar t_1)) \tag{3.2}$$

and

$$0 \leq \mathbf{N}_\mathbf{r}(t_1) \leq \mathbf{N}_\mathbf{r}(0)\exp(-(\upsilon_\mathbf{r} + \chi_\mathbf{r})t_1) + \frac{\chi_\hbar}{\upsilon_\hbar}(1 - \exp(-(\upsilon_\mathbf{r} + \chi_\mathbf{r})t_1)). \tag{3.3}$$

This gives the desired estimates.

3.2. Disease free equilibrium for $\mathbb{MPX}$ virus

The disease-free phases are cohorts $\mathbf{S}_\hbar, \mathbf{R}_\hbar$ *and* $\mathbf{S}_\mathbf{r}$, in our developed framework (2.5), while the infectious category includes compartments $\mathbf{E}_\hbar, \mathbf{I}_\hbar, \mathbf{Q}_\hbar, \mathbf{E}_\mathbf{r}$ *and* $\mathbf{I}_{r_1}$.

As a result, the $\mathbb{MPX}$-free equilibrium condition can be determined as $E_0 = \left(\frac{\chi_\hbar}{\upsilon_\hbar}, 0, 0, 0, 0, \frac{\chi_\mathbf{r}}{\upsilon_\mathbf{r}}, 0, 0\right)$.

3.3. Basic reproduction number

One of the major considerations for analyzing an epidemic's protracted dynamics is the basic reproduction number. It is the number of additional occurrences created by a single infectious person over the course of their pathogenic agent's lifetime. To obtain the formulation of the reproducing number $\mathbb{R}_0$, we used the next-generation matrix procedure described in [50]. It was initially mentioned in [51], which goes into great length about how to estimate $\mathbb{R}_0$ using this approach. There are also several publications on this research wherein the authors describe a next-generation matrix approach to determine the basic reproduction number representation.

The matrix $\mathcal{F}$ corresponds to transmissions and the matrix $\mathcal{V}$ to transitions. In this paper, we include death in the transition matrix to keep the notation simple (in contrast with Diekmann et al. [50]). Hence, all epidemiological events that lead to new infections are incorporated into the model via $\mathcal{F}$, and all other events via $\mathcal{V}$. Progress to either death or immunity guarantees that $\mathcal{V}$ is invertible. Thus, the $\mathbb{MPX}$ can be expressed as

$$\mathcal{F} = \begin{bmatrix} 0 \\ \frac{\eta_1 \mathbf{I_r} + \eta_2 \mathbf{I}_\hbar}{\mathbf{N}_\hbar} \mathbf{S}_\hbar \\ 0 \\ 0 \\ 0 \\ 0 \\ 0 \\ 0 \\ 0 \end{bmatrix} \quad \textit{and} \quad \mathcal{V} = \begin{bmatrix} -\chi_\hbar + \frac{(\eta_1 \mathbf{I_r} + \eta_2 \mathbf{I}_\hbar)\mathbf{S}_\hbar}{\mathbf{N}_\hbar} + \upsilon_\hbar \mathbf{S}_\hbar - \sigma \mathbf{Q}_\hbar \\ (\delta_1 + \delta_2 + \upsilon_\hbar)\mathbf{E}_\hbar \\ -\delta_1 \mathbf{E}_\hbar + (\upsilon_\hbar + \varphi_\hbar + \gamma)\mathbf{I}_\hbar \\ -\delta_2 \mathbf{E}_\hbar + (\sigma + \upsilon_\hbar + \varphi_\hbar + \psi)\mathbf{Q}_\hbar \\ -\gamma \mathbf{I}_\hbar - \psi \mathbf{Q}_\hbar + \upsilon_\hbar \mathbf{R}_\hbar \\ -\chi_{\mathbf{r}} - \frac{\eta_3 \mathbf{S_r} \mathbf{I_r}}{\mathbf{N_r}} + \upsilon_{\mathbf{r}} \mathbf{S_r} \\ -\frac{\eta_3 \mathbf{S_r} \mathbf{I_r}}{\mathbf{N_r}} + (\upsilon_{\mathbf{r}} + \delta_3)\mathbf{E_r} \\ -\delta_3 \mathbf{E_r} + (\upsilon_{\mathbf{r}} + \varphi_{\mathbf{r}})\mathbf{I_r} \end{bmatrix}.$$

The progression of contaminated individuals from $\mathbf{E}_\hbar$ to $\mathbf{E}_\hbar$ or $\mathbf{Q}_\hbar$ is not considered as the emergence of a new virus, but rather the evolution of contaminated individuals across multiple cohorts. So, we have a linearized system at a disease-free state:

$$\mathbf{F} = \begin{bmatrix} 0 & \eta_2 & 0 & \eta_1 \\ 0 & 0 & 0 & 0 \\ 0 & 0 & 0 & 0 \\ 0 & 0 & 0 & 0 \end{bmatrix} \quad \textit{and} \quad \mathbf{V} = \begin{bmatrix} (\delta_1 + \delta_2 + \upsilon_\hbar) & 0 & 0 & 0 \\ -\delta_1 & \upsilon_\hbar + \varphi_\hbar + \gamma & 0 & 0 \\ -\delta_2 & 0 & \sigma + \psi + \varphi_\hbar + \upsilon_\hbar & 0 \\ 0 & 0 & 0 & \upsilon_{\mathbf{r}} + \varphi_{\mathbf{r}} \end{bmatrix},$$

where $\mathbf{F}$ and $\mathbf{V}$ are 4×4 matrices, computed as $\mathbf{F} = \frac{\partial \mathcal{F}_J}{\partial x_j}$ and $\mathbf{V} = \frac{\partial \mathcal{V}_J}{\partial x_j}$. For the sake of convenience, assume $b_1 = \delta_1 + \delta_2 + \upsilon_\hbar$, $b_2 = \upsilon_\hbar + \varphi_\hbar + \gamma$, $b_3 = \sigma + \psi + \varphi_\hbar + \upsilon_\hbar$ and $b_4 = \upsilon_{\mathbf{r}} + \varphi_{\mathbf{r}}$.

Furthermore, the next-generation matrix is presented as:

$$\mathbf{FV^{-1}} = \frac{1}{b_1 b_2 b_3 b_4} \begin{bmatrix} \eta_2 \delta_1 b_3 b_4 & 0 & 0 & \eta_1 b_1 b_2 b_3 \\ 0 & 0 & 0 & 0 \\ 0 & 0 & 0 & 0 \\ 0 & 0 & 0 & 0 \end{bmatrix}.$$

Thus, the reproductive number for System (2.5) can be calculated as

$$\mathbb{R}_0 = \Psi(\mathbf{FV^{-1}}) = \frac{\eta_2 \delta_1 b_3 b_4}{b_1 b_2 b_3 b_4},$$

or equivalently,

$$\mathbb{R}_0 = \frac{\eta_2\delta_1}{(\delta_1+\delta_2+\upsilon_\hbar)(\upsilon_\hbar+\varphi_\hbar+\gamma)}.$$

3.4. Local stability of disease-free equilibrium

Theorem 3.1. *Suppose there is two non-negative integers* ϑ_1, ϑ_2 *with* $gcd(\vartheta_1, \vartheta_2) = 1$, $\sigma = \vartheta_1/\vartheta_2$ *and* $K = \vartheta_1$*; then, the model* (3.1) *is locally asymptotically stable if* $|Arg(\lambda)| > \frac{\pi}{2K}$ *for all roots of the concerning equation* $\det(diag(\lambda^{K\sigma}) - \mathbb{J}(E_0)) = 0$.

Proof. The Jacobian matrix of system (3.1) at E_0 implies,

$$(\mathbf{J}_0)_{E_0} = \begin{bmatrix} -\upsilon_\hbar & 0 & -\eta_2 & 0 & 0 & 0 & 0 & -\eta_1 \\ 0 & -B_1 & \eta_2 & 0 & 0 & 0 & 0 & \eta_1 \\ 0 & \delta_1 & -B_2 & 0 & 0 & 0 & 0 & 0 \\ 0 & \delta_2 & 0 & -B_3 & 0 & 0 & 0 & 0 \\ 0 & 0 & \gamma & \psi & -\upsilon_\hbar & 0 & 0 & 0 \\ 0 & 0 & 0 & 0 & 0 & -\upsilon_{\mathbf{r}} & 0 & 0 \\ 0 & 0 & 0 & 0 & 0 & 0 & -B_4 & \eta_3 \\ 0 & 0 & 0 & 0 & 0 & 0 & \eta_3 & -B_5 \end{bmatrix} \tag{3.4}$$

Suppose the concerned eigenvalues are $\varpi = (\varpi_1, \varpi_2, \varpi_3, \varpi_4, \varpi_5, \varpi_6, \varpi_7, \varpi_8)$. This can be achieved by simple computation:

$$\begin{aligned} &-\upsilon_\hbar\varpi_1 - \eta_2\varpi_3 - \eta_1\eta_8 = 0, \ -B_1\varpi_2 + \eta_2\varpi_3 + \eta_1\varpi_8 = 0, \ \delta_1\varpi_2 - B_2\varpi_3 = 0, \\ &\delta_2\varpi_2 - B_3\varpi_4 = 0, \ \gamma\varpi_3 + \psi\varpi_4 - \upsilon_\hbar\varpi_5 = 0, \ \upsilon_{\mathbf{r}}\varpi_6 - \eta_3\varpi_8 = 0, \ -B_4\varpi_7 + \eta_3\varpi_8 = 0, \\ &\delta_3\varpi_7 - B_5\varpi_8 = 0. \end{aligned} \tag{3.5}$$

Clearly, ϖ_J, $J = 1, 2, ..., 8$ are positive if $\mathbb{R}_0 < 1$. Moreover, the argument is

$$\arg(\varpi_J) = \frac{\pi}{\vartheta_1} + J\frac{2\pi}{\vartheta_1} > \frac{\pi}{K} > \frac{\pi}{2K}, \ J = 0, 1, 2, ...(\vartheta_1 - 1).$$

The arguments of the other roots can be acquired in a similar way and are all greater than $\frac{\pi}{2K}$ if $\mathbb{R}_0 < 1$. So, the DFE is locally asymptotically stable for $\mathbb{R}_0 < 1$.

Further, we adopted the methodology proposed by Castillo-Chavez and Song [52] to determine the requirements for global stability (GS) for E_0, which stipulates that the model scheme be stated in the appropriate pattern:

$$\begin{aligned} \dot{X}_1 &= F_1(X_1, Z_1), \\ \dot{Z}_1 &= G_1(X_1, Z_1), G_1(X_1, 0) = 0. \end{aligned} \tag{3.6}$$

Now, $X_1 \in \mathbb{R}^n$ represents the unexposed persons and $Z_1 \in \mathbb{R}^m$ states the infectious people. Using this terminology, the DFE is calculated by $H_0 = (X_{10}, 0)$. The GS of the DFE is now guaranteed by the underlying two requirements:

a) *For* $\dot{X}_1 = F_1(X_1, 0),\ X_{10}$ is asymptotically GS.
b) $G_1 = (X_1, Z_1) = A_1 Z_1 - \tilde{G}_1(X_1, Z_1)$, where $\tilde{G}_1(X_1, Z_1) \geq 0$ for $X_1, Z_1 \in \Upsilon$.
Since $A_1 = D_{Z_1} G_1(X_{10}, 0)$ is an M-matrix and the viability of the system is presented by Υ. The GS of E_0 is then determined by the accompanying lemma.

Lemma 3.2. *Suppose there is an equilibrium point* $H_0 = (X_{10}, 0)$ *that is asymptotically GS when* $\mathbb{R}_0 < 1$ *admits the assertions* (***a***) *and* (***b***).

Proof. Firstly, we intend to verify **a)** as:

$$F_1(X_1, 0) = \begin{bmatrix} \chi_\hbar - \upsilon_\hbar \mathbf{S}_\hbar \\ -\upsilon_\hbar \mathbf{R}_\hbar \\ \chi_\mathbf{r} - \upsilon_\mathbf{r} \mathbf{S}_\mathbf{r} \\ -(\upsilon_\mathbf{r} + \delta_3)\mathbf{E}_\mathbf{r} \end{bmatrix}.$$

The characteristic polynomial of $F_1(X_1, 0)$ implies that $\lambda_1 = \lambda_2 = -\upsilon_\hbar,\ \lambda_3 = -\upsilon_\mathbf{r}$ *and* $\lambda_4 = -\upsilon_\mathbf{r} - \delta_3$. Therefore, $X_1 = X_{10}$ is asymptotically GS.
Furthermore, we have

$$G_1(X_1, Z_1) = A_1 Z_1 - \tilde{G}_1(X_1, Z_1) = \begin{bmatrix} -b_1 & \frac{\eta_2 \mathbf{S}^0_\hbar}{\mathbf{N}_\hbar} & 0 & \frac{\eta_1 \mathbf{S}^0_\hbar}{\mathbf{N}_\hbar} \\ \delta_1 & -b_2 & 0 & 0 \\ \delta_2 & 0 & -b_3 & 0 \\ 0 & 0 & 0 & b_4 \end{bmatrix} \begin{bmatrix} \mathbf{E}_\hbar \\ \mathbf{I}_\hbar \\ \mathbf{Q}_\hbar \\ \mathbf{I}_\mathbf{r} \end{bmatrix} - \begin{bmatrix} \frac{\eta_2(\mathbf{S}^0_\hbar - \mathbf{S}_\hbar) + \eta_1(\mathbf{S}^0_\hbar - \mathbf{S}_\hbar)}{\mathbf{N}_\hbar} \mathbf{E}_\hbar \\ 0 \\ 0 \\ \delta_3 \mathbf{E}_\mathbf{r} \end{bmatrix}.$$

As a result, it is clear that A_1 satisfies all of the criteria stated in **b)**.

3.5. Endemic equilibrium point (EEP)

The EEP happens when the illness continues to spread among the community, as indicated by

$$\mathbf{E}^*_0 = (\mathbf{S}^*_\hbar, \mathbf{E}^*_\hbar, \mathbf{I}^*_\hbar, \mathbf{Q}^*_\hbar, \mathbf{R}^*_\hbar, \mathbf{S}^*_\mathbf{r}, \mathbf{E}^*_\mathbf{r}, \mathbf{I}^*_\mathbf{r}).$$

Thus, we have

$$\begin{aligned} \mathbf{E}^*_0 \quad = \Big(& \frac{b_1 b_3 \chi_\hbar}{\upsilon_\hbar b_1 b_3 - \delta_2 \sigma b_6 + b_1 b_3 b_6}, \ \frac{b_6 b_3 \chi_\hbar}{\upsilon_\hbar b_1 b_3 - \delta_2 \sigma b_6 + b_1 b_3 b_6}, \ \frac{\delta_1 b_3 b_6 \chi_\hbar}{b_2(\upsilon_\hbar b_1 b_3 - \delta_3 \sigma b_6 + b_1 b_3 b_6)} \\ & , \ \frac{\delta_2 b_6 \chi_\hbar}{\upsilon_\hbar b_1 b_3 - \delta_3 \sigma b_6 + b_1 b_3 b_6}, \ \frac{(\delta_1 \gamma b_3 + \delta_2 b_2 \psi) b_6 \chi_\hbar}{\upsilon_\hbar b_2(\upsilon_\hbar b_1 b_3 - \delta_3 \sigma b_6 + b_1 b_3 b_6)}, \ \frac{\chi_\mathbf{r}}{\upsilon_\mathbf{r} + b_7}, \ \frac{\chi_\mathbf{r}}{b_5(\upsilon_\mathbf{r} + b_7)}, \ \frac{b_7 \delta - 3\chi_\mathbf{r}}{b_4 b_5(\upsilon_\mathbf{r} + b_7)} \Big), \end{aligned} \tag{3.7}$$

where $b_5 = \upsilon_\mathbf{r} + \delta_3,\ \ b_6 = \frac{\eta_1 \mathbf{I}^*_\mathbf{r} + \eta_2 \mathbf{I}^*_\hbar}{\mathbf{N}_\hbar}$ *and* $b_7 = \frac{\eta_3 \mathbf{I}^*_\mathbf{r}}{\mathbf{N}_\mathbf{r}}$

3.6. Stability of the EE

Here, the Routh–Hurwitz threshold [53] will be employed to demonstrate the endemic equilibrium's (EE's) local stability. The criteria whereby the EE is locally asymptotically stable will be determined

by the Jacobian matrix as

$$\mathbb{J} = \begin{bmatrix} \varrho_{11} & 0 & \varrho_{13} & \varrho_{14} & 0 & 0 & 0 & \varrho_{18} \\ \varrho_{21} & \varrho_{22} & \varrho_{23} & 0 & 0 & 0 & 0 & \varrho_{28} \\ 0 & \varrho_{32} & \varrho_{33} & 0 & 0 & 0 & 0 & 0 \\ 0 & \varrho_{42} & 0 & \varrho_{44} & 0 & 0 & 0 & 0 \\ 0 & 0 & \varrho_{53} & \varrho_{54} & \varrho_{55} & 0 & 0 & 0 \\ 0 & 0 & 0 & 0 & 0 & \varrho_{66} & 0 & \varrho_{68} \\ 0 & 0 & 0 & 0 & 0 & \varrho_{76} & \varrho_{77} & \varrho_{78} \\ 0 & 0 & 0 & 0 & 0 & 0 & \varrho_{87} & \varrho_{88} \end{bmatrix}, \tag{3.8}$$

where $\varrho_{11} = -\frac{\eta_1 \mathbf{I_r} + \eta_2 \mathbf{I}_\hbar}{\mathbf{N}_\hbar}$, $\varrho_{13} = -\frac{\eta_2 \mathbf{S}_\hbar}{\mathbf{N}_\hbar}$, $\varrho_{14} = \phi$, $\varrho_{18} = -\frac{\eta_1 \mathbf{S}_\hbar}{\mathbf{N}_\hbar}$,
$\varrho_{21} = -\frac{\eta_1 \mathbf{I_r} + \eta_2 \mathbf{I}_\hbar}{\mathbf{N}_\hbar}$, $\varrho_{22} = -b_1$, $\varrho_{23} = \frac{\eta_2 \mathbf{S}_\hbar}{\mathbf{N}_\hbar}$, $\varrho_{28} = \frac{\eta_1 \mathbf{I}_\hbar}{\mathbf{N}_\hbar}$, $\varrho_{32} = \delta_1$, $\varrho_{33} = -(\upsilon_\hbar + \varphi_\hbar + \gamma)$, $\varrho_{42} = \delta_2$, $\varrho_{44} = -b_2$, $\varrho_{53} = \gamma$, $\varrho_{54} = \psi$, $\varrho_{55} = -\upsilon_\hbar$, $\varrho_{66} = -\left(\upsilon_{\mathbf{r}} + \frac{\eta_3 \mathbf{I_r}}{\mathbf{N_r}}\right)$, $\varrho_{68} = -\frac{\eta_3 \mathbf{S_r}}{\mathbf{N_r}}$, $\varrho_{76} = \frac{\eta_3 \mathbf{I_r}}{\mathbf{N_r}}$, $\varrho_{77} = -b_5$, $\varrho_{78} = \frac{\eta_3 \mathbf{S_r}}{\mathbf{N_r}}$, $\varrho_{87} = \delta_3$ *and* $\varrho_{88} = -b_4$. The characteristic equation yields

$$y_1^8 + B_1 y_1^7 + B_2 y_1^6 + B_3 y_1^5 + B_4 y_1^4 + B_5 y_1^3 + B_6 y_1^2 + B_7 y_1 + B_8 = 0, \tag{3.9}$$

where B_J, $J = 0, 1, 2, ..., 8$ are the coefficients of y_1^J after the polynomial has been converted to the simplified form.

We shall use the appropriate adjustment to achieve the EE stability requirements:

$$\begin{aligned} &\mathcal{P} = \frac{B_1 B_2 - B_0 B_3}{B_1},\ \mathcal{Q} = \frac{B_1 B_4 - B_0 B_5}{B_1},\ \mathcal{R} = \frac{B_1 B_6 - B_0 B_7}{B_1}, \\ &\mathcal{S} = B_8,\ \mathcal{P}^* = \frac{\mathcal{P} B_3 - \mathcal{Q} B_1}{\mathcal{P}},\ \mathcal{Q}^* = \frac{\mathcal{P} B_5 - \mathcal{R} B_1}{\mathcal{P}},\ \mathcal{R}^* = \frac{\mathcal{P} B_7 - \mathcal{S} B_1}{\mathcal{P}}, \\ &\mathcal{M} = \frac{\mathcal{P}^* \mathcal{Q} - \mathcal{P} \mathcal{Q}^*}{\mathcal{P}^*},\ \mathcal{N} = \frac{\mathcal{P}^* \mathcal{R} - \mathcal{P} \mathcal{R}^*}{\mathcal{P}^*},\ \mathcal{T} = \frac{\mathcal{P}^* \mathcal{S}}{\mathcal{P}^*},\ \mathcal{M}^* = \frac{\mathcal{M} \mathcal{Q}^* - \mathcal{N} \mathcal{P}^*}{\mathcal{M}}, \\ &\mathcal{N}^* = \frac{\mathcal{M} \mathcal{R}^* - \mathcal{T} \mathcal{P}^*}{\mathcal{M}},\ \mathcal{X}^* = \frac{\mathcal{N} \mathcal{M}^* - \mathcal{M} \mathcal{N}^*}{\mathcal{M}^*} \end{aligned} \tag{3.10}$$

Therefore, the Hurwitz assumptions concerning the characteristic equation are

$$\begin{aligned} &B_1 > 0, \\ &B_1 B_2 > B_3, \\ &B_1 B_2 B_3 + B_0 B_1 B_5 > B_0 B_3^2 + B_4 B_1^2, \\ &\mathcal{P}^* \mathcal{Q} > \mathcal{P} \mathcal{Q}^*,\ \mathcal{Q}^* \mathcal{M} > \mathcal{N} \mathcal{P}^*,\ \mathcal{M}^* \mathcal{N} > \mathcal{M} \mathcal{N}^{*,}\ \mathcal{N}^* \mathcal{X} > \mathcal{T} \mathcal{M}^*. \end{aligned} \tag{3.11}$$

Hence, the EEP is locally asymptotic stable.

3.7. Model design

The combination of the DEs depicts the intricate framework (2.5), which includes the assumptions, the saturation contact pattern, and the schematic diagram shown in Figure 3, as well as analyses of the

concept (2.5) using the ABC fractional derivative.

$$\begin{cases} {}^{ABC}_{0}\mathbf{D}^{\rho}_{\tau}\mathbf{S}_{\hbar}(\tau) = \Omega_1(\tau, \mathbf{S}_{\hbar}), \\ {}^{ABC}_{0}\mathbf{D}^{\rho}_{\tau}\mathbf{E}_{\hbar}(\tau) = \Omega_2(\tau, \mathbf{E}_{\hbar}), \\ {}^{ABC}_{0}\mathbf{D}^{\rho}_{\tau}\mathbf{I}_{\hbar}(\tau) = \Omega_3(t_3, \mathbf{I}_{\hbar}), \\ {}^{ABC}_{0}\mathbf{D}^{\rho}_{\tau}\mathbf{Q}_{\hbar}(\tau) = \Omega_4(\tau, \mathbf{Q}_{\hbar}), \\ {}^{ABC}_{0}\mathbf{D}^{\rho}_{\tau}\mathbf{R}_{\hbar}(\tau) = \Omega_5(\tau, \mathbf{R}_{\hbar}), \\ {}^{ABC}_{0}\mathbf{D}^{\rho}_{\tau}\mathbf{S}_{\mathbf{r}}(\tau) = \Omega_6(\tau, \mathbf{S}_{\mathbf{r}}), \\ {}^{ABC}_{0}\mathbf{D}^{\rho}_{\tau}\mathbf{E}_{\mathbf{r}}(\tau) = \Omega_7(\tau, \mathbf{Q}_{\hbar}), \\ {}^{ABC}_{0}\mathbf{D}^{\rho}_{\tau}\mathbf{I}_{\mathbf{r}}(\tau) = \Omega_8(\tau, \mathbf{Q}_{\hbar}), \end{cases} \tag{3.12}$$

where kernels are configured as shown in:

$$\begin{cases} \Omega_1(\tau, \mathbf{S}_{\hbar}) = \chi_{\hbar} - \frac{(\eta_1\mathbf{I}_{\mathbf{r}} + \eta_2\mathbf{I}_{\hbar})\mathbf{S}_{\hbar}}{\mathbf{N}_{\hbar}} - \upsilon_{\hbar}\mathbf{S}_{\hbar} + \sigma\mathbf{Q}_{\hbar}, \\ \Omega_2(\tau, \mathbf{E}_{\hbar}) = \frac{(\eta_1\mathbf{I}_{\mathbf{r}} + \eta_2\mathbf{I}_{\hbar})\mathbf{S}_{\hbar}}{\mathbf{N}_{\hbar}} - (\delta_1 + \delta_2 + \upsilon_{\hbar})\mathbf{E}_{\hbar}, \\ \Omega_3(\tau, \mathbf{I}_{\hbar}) = \delta_1\mathbf{E}_{\hbar} - (\upsilon_{\hbar} + \varphi_{\hbar} + \gamma)\mathbf{I}_{\hbar}, \\ \Omega_4(\tau, \mathbf{Q}_{\hbar}) = \delta_2\mathbf{E}_{\hbar} - (\sigma + \upsilon_{\hbar} + \varphi_{\hbar} + \psi)\mathbf{Q}_{\hbar}, \\ \Omega_5(\tau, \mathbf{R}_{\hbar}) = \gamma\mathbf{I}_{\hbar} + \psi\mathbf{Q}_{\hbar} - \upsilon_{\hbar}\mathbf{R}_{\hbar}, \\ \Omega_6(\tau, \mathbf{S}_{\mathbf{r}}) = \chi_{\mathbf{r}} - \frac{\eta_3\mathbf{S}_{\mathbf{r}}\mathbf{I}_{\mathbf{r}}}{\mathbf{N}_{\mathbf{r}}} - \upsilon_{\mathbf{r}}\mathbf{S}_{\mathbf{r}}, \\ \Omega_7(\tau, \mathbf{E}_{\mathbf{r}}) = \frac{\eta_3\mathbf{S}_{\mathbf{r}}\mathbf{I}_{\mathbf{r}}}{\mathbf{N}_{\mathbf{r}}} - (\upsilon_{\mathbf{r}} + \delta_3)\mathbf{E}_{\mathbf{r}}, \\ \Omega_8(\tau, \mathbf{I}_{\mathbf{r}}) = \delta_3\mathbf{E}_{\mathbf{r}} - (\upsilon_{\mathbf{r}} + \varphi_{\mathbf{r}})\mathbf{I}_{\mathbf{r}}, \end{cases} \tag{3.13}$$

which are subject the following ICs: $\mathbf{S}_{\hbar}(0) = \mathbf{S}_{\hbar 0},\ \mathbf{E}_{\hbar}(0) = \mathbf{E}_{\hbar 0}, \mathbf{I}_{\hbar}(0) = \mathbf{I}_{\hbar 0}, \mathbf{Q}_{\hbar}(0) = \mathbf{Q}_{\hbar 0}, \mathbf{R}_{\hbar}(0) = \mathbf{R}_{\hbar 0}, \mathbf{S}_{\mathbf{r}}(0) = \mathbf{S}_{\mathbf{r}0},\ \mathbf{E}_{\mathbf{r}}(0) = \mathbf{E}_{\mathbf{r}0}$ *and* $\mathbf{I}_{\mathbf{r}}(0) = \mathbf{I}_{\mathbf{r}0}$.

Here, we have $d\mathbf{N}/d\tau = \chi_{\hbar} - \varphi_{\hbar}\mathbf{I}_{\hbar} - \upsilon_{\hbar}\mathbf{N}_{\hbar}$ in the occurrence of human infectious and rodent $d\mathbf{N}/d\tau = \mathbf{S}_{\mathbf{r}} + \mathbf{E}_{\mathbf{r}} + \mathbf{I}_{\mathbf{r}}$, illustrating that the size of the communities is not constant. The parameters that were evaluated in the investigation (2.5) are listed in Table 1.

3.8. Existence–uniqueness results for $\mathbb{MPX}$ model

The Banach fixed point $\tilde{f}_p$ assumption for contraction mapping is used to demonstrate the existence–uniqueness of the result for the ABC fractional framework stated in (3.12). It is vital to understand the two new theories preceding the progress on [43].

To establish the system's existence-uniqueness, we proceed as follows. While implementing the

Atangana-Baleanu fractional integral, we can obtain System (3.12):

$$\begin{cases} \mathbf{S}_{\hbar}(\tau)-\mathbf{S}_{\hbar}(0)=\frac{1-\rho}{\mathbb{ABC}(\rho)}\Omega_1(\tau,\mathbf{S}_{\hbar})+\frac{\rho}{\mathbb{ABC}(\rho)\Gamma(\rho)}\int_0^{\tau}\Omega_1(\varsigma,\mathbf{S}_{\hbar})(\tau-\varsigma)^{\rho-1}d\varsigma,\\ \mathbf{E}_{\hbar}(\tau)-\mathbf{E}_{\hbar}(0)=\frac{1-\rho}{\mathbb{ABC}(\rho)}\Omega_2(\tau,\mathbf{E}_{\hbar})+\frac{\rho}{\mathbb{ABC}(\rho)\Gamma(\rho)}\int_0^{\tau}\Omega_2(\varsigma,\mathbf{E}_{\hbar})(\tau-\varsigma)^{\rho-1}d\varsigma,\\ \mathbf{I}_{\hbar}(\tau)-\mathbf{I}_{\hbar}(0)=\frac{1-\rho}{\mathbb{ABC}(\rho)}\Omega_3(\tau,\mathbf{I}_{\hbar})+\frac{\rho}{\mathbb{ABC}(\rho)\Gamma(\rho)}\int_0^{\tau}\Omega_3(\varsigma,\mathbf{I}_{\hbar})(\tau-\varsigma)^{\rho-1}d\varsigma,\\ \mathbf{Q}_{\hbar}(\tau)-\mathbf{Q}_{\hbar}(0)=\frac{1-\rho}{\mathbb{ABC}(\rho)}\Omega_4(\tau,\mathbf{Q}_{\hbar})+\frac{\rho}{\mathbb{ABC}(\rho)\Gamma(\rho)}\int_0^{\tau}\Omega_4(\varsigma,\mathbf{Q}_{\hbar})(\tau-\varsigma)^{\rho-1}d\varsigma,\\ \mathbf{R}_{\hbar}(\tau)-\mathbf{R}_{\hbar}(0)=\frac{1-\rho}{\mathbb{ABC}(\rho)}\Omega_5(\tau,\mathbf{R}_{\hbar})+\frac{\rho}{\mathbb{ABC}(\rho)\Gamma(\rho)}\int_0^{\tau}\Omega_5(\varsigma,\mathbf{R}_{\hbar})(\tau-\varsigma)^{\rho-1}d\varsigma,\\ \mathbf{S}_{\mathbf{r}}(\tau)-\mathbf{S}_{\mathbf{r}}(0)=\frac{1-\rho}{\mathbb{ABC}(\rho)}\Omega_6(\tau,\mathbf{R}_{\hbar})+\frac{\rho}{\mathbb{ABC}(\rho)\Gamma(\rho)}\int_0^{\tau}\Omega_6(\varsigma,\mathbf{R}_{\hbar})(\tau-\varsigma)^{\rho-1}d\varsigma,\\ \mathbf{E}_{\mathbf{r}}(\tau)-\mathbf{E}_{\mathbf{r}}(0)=\frac{1-\rho}{\mathbb{ABC}(\rho)}\Omega_7(\tau,\mathbf{E}_{\mathbf{r}})+\frac{\rho}{\mathbb{ABC}(\rho)\Gamma(\rho)}\int_0^{\tau}\Omega_7(\varsigma,\mathbf{E}_{\mathbf{r}})(\tau-\varsigma)^{\rho-1}d\varsigma,\\ \mathbf{I}_{\mathbf{r}}(\tau)-\mathbf{I}_{\mathbf{r}}(0)=\frac{1-\rho}{\mathbb{ABC}(\rho)}\Omega_8(\tau,\mathbf{I}_{\mathbf{r}})+\frac{\rho}{\mathbb{ABC}(\rho)\Gamma(\rho)}\int_0^{\tau}\Omega_8(\varsigma,\mathbf{I}_{\mathbf{r}})(\tau-\varsigma)^{\rho-1}d\varsigma. \end{cases} \tag{3.14}$$

Assume that the collection $\mathfrak{B}=\Lambda(\mathfrak{J})\times\Lambda(\mathfrak{J})\times\Lambda(\mathfrak{J})\times\Lambda(\mathfrak{J})\times\Lambda(\mathfrak{J})\times\Lambda(\mathfrak{J})\times\Lambda(\mathfrak{J})\times\Lambda(\mathfrak{J})$, where $\Lambda(\mathfrak{J})=\mathbf{C}[0,\bar{T}]$ refers to real-valued continuous functions for the $\mathfrak{B}$ on $\mathfrak{J}=[0,\bar{T}]$, taking into account the established norm $\left\|(\mathbf{S}_{\hbar},\mathbf{E}_{\hbar},\mathbf{I}_{\hbar},\mathbf{Q}_{\hbar},\mathbf{R}_{\hbar},\mathbf{S}_{\mathbf{r}},\mathbf{E}_{\mathbf{r}},\mathbf{I}_{\mathbf{r}})\right\|=\left\|\mathbf{S}_{\hbar}\right\|+\left\|\mathbf{E}_{\hbar}\right\|+\left\|\mathbf{I}_{\hbar}\right\|+\left\|\mathbf{Q}_{\hbar}\right\|+\left\|\mathbf{R}_{\hbar}\right\|+\left\|\mathbf{S}_{\mathbf{r}}\right\|+\left\|\mathbf{E}_{\mathbf{r}}\right\|+\left\|\mathbf{I}_{\mathbf{r}}\right\|$, where $\left\|\mathbf{S}_{\hbar}\right\|=\sup_{\tau\in\mathfrak{J}}\left|\mathbf{S}_{\hbar}(\tau)\right|$, $\left\|\mathbf{E}_{\hbar}\right\|=\sup_{\tau\in\mathfrak{J}}\left|\mathbf{E}_{\hbar}(\tau)\right|$, $\left\|\mathbf{I}_{\hbar}\right\|=\sup_{\tau\in\mathfrak{J}}\left|\mathbf{I}_{\hbar}(\tau)\right|$, $\left\|\mathbf{Q}_{\hbar}\right\|=\sup_{\tau\in\mathfrak{J}}\left|\mathbf{Q}_{\hbar}(\tau)\right|$, $\left\|\mathbf{R}_{\hbar}\right\|=\sup_{\tau\in\mathfrak{J}}\left|\mathbf{R}_{\hbar}(\tau)\right|$, $\left\|\mathbf{S}_{\mathbf{r}}\right\|=\sup_{\tau\in\mathfrak{J}}\left|\mathbf{S}_{\mathbf{r}}(\tau)\right|$, $\left\|\mathbf{E}_{\mathbf{r}}\right\|=\sup_{\tau\in\mathfrak{J}}\left|\mathbf{E}_{\mathbf{r}}(\tau)\right|$ and $\left\|\mathbf{I}_{\mathbf{r}}\right\|=\sup_{\tau\in\mathfrak{J}}\left|\mathbf{I}_{\mathbf{r}}(\tau)\right|$.

The accompanying result is established on the basis of the contraction and the Lipschitz supposition.

Theorem 3.2. *For kernels* $\Omega_{\ell},\ \ell=1,2,...,8$ *in* (3.12)*, there exists* $\mathbb{L}_{\ell}>0,\ \ell=1,2,...8$*, such that*

$$\begin{cases} \left\|\Omega_1(\tau,\mathbf{S}_{\hbar})-\Omega_1(\tau,\mathbf{S}_{\hbar 1})\right\|\leq\mathbb{L}_1\left\|\mathbf{S}_{\hbar}(\tau)-\mathbf{S}_{\hbar 1}(\tau)\right\|,\\ \left\|\Omega_2(\tau,\mathbf{E}_{\hbar})-\Omega_2(\tau,\mathbf{E}_{\hbar 1})\right\|\leq\mathbb{L}_2\left\|\mathbf{E}_{\hbar}(\tau)-\mathbf{E}_{\hbar 1}(\tau)\right\|,\\ \left\|\Omega_3(\tau,\mathbf{I}_{\hbar})-\Omega_3(\tau,\mathbf{I}_{\hbar_1})\right\|\leq\mathbb{L}_3\left\|\mathbf{I}_{\hbar}(\tau)-\mathbf{I}_{\hbar_1}(\tau)\right\|,\\ \left\|\Omega_4(\tau,\mathbf{Q}_{\hbar})-\Omega_4(\tau,\mathbf{Q}_{\hbar 1})\right\|\leq\mathbb{L}_4\left\|\mathbf{Q}_{\hbar}(\tau)-\mathbf{Q}_{\hbar_1}(\tau)\right\|,\\ \left\|\Omega_5(\tau,\mathbf{R}_{\hbar})-\Omega_5(\tau,\mathbf{R}_{\hbar 1})\right\|\leq\mathbb{L}_5\left\|\mathbf{R}_{\hbar}(\tau)-\mathbf{R}_{\hbar_1}(\tau)\right\|,\\ \left\|\Omega_6(\tau,\mathbf{S}_{\mathbf{r}})-\Omega_6(\tau,\mathbf{S}_{m11})\right\|\leq\mathbb{L}_6\left\|\mathbf{S}_{\mathbf{r}}(\tau)-\mathbf{S}_{m11}(\tau)\right\|,\\ \left\|\Omega_7(\tau,\mathbf{E}_{\mathbf{r}})-\Omega_7(\tau,\mathbf{E}_{\mathbf{r}1})\right\|\leq\mathbb{L}_7\left\|\mathbf{E}_{\mathbf{r}}(\tau)-\mathbf{E}_{\mathbf{r}1}(\tau)\right\|,\\ \left\|\Omega_8(\tau,\mathbf{I}_{\mathbf{r}})-\Omega_8(\tau,\mathbf{I}_{\mathbf{r}1})\right\|\leq\mathbb{L}_8\left\|\mathbf{I}_{\mathbf{r}}(\tau)-\mathbf{I}_{\mathbf{r}1}(\tau)\right\|, \end{cases} \tag{3.15}$$

which are contractions for $\mathbb{L}_{\ell}\in[0,1),\ \ell=1,2,...,8$.

Proof. To achieve Lipschitz's requirements, we have

$$\begin{aligned} \left\|\Omega_1(\tau,\mathbf{S}_{\hbar})-\Omega_1(\tau,\mathbf{S}_{\hbar 1})\right\| &= \left\|\chi_{\hbar}-\frac{(\eta_1\mathbf{I}_{\mathbf{r}}+\eta_2\mathbf{I}_{\hbar})\mathbf{S}_{\hbar}}{\mathbf{N}_{\hbar}}-\upsilon_{\hbar}\mathbf{S}_{\hbar}+\sigma\mathbf{Q}_{\hbar}\right.\\ &\quad\left.-\Big(\chi_{\hbar}-\frac{(\eta_1\mathbf{I}_{\mathbf{r}}+\eta_2\mathbf{I}_{\hbar})\mathbf{S}_{\hbar_1}}{\mathbf{N}_{\hbar}}-\upsilon_{\hbar}\mathbf{S}_{\hbar_1}+\sigma\mathbf{Q}_{\hbar}\Big)\right\|\\ &= \left\|-\Big(\frac{(\eta_1\mathbf{I}_{\mathbf{r}}+\eta_2\mathbf{I}_{\hbar})}{\mathbf{N}_{\hbar}}+\upsilon_{\hbar}\Big)(\mathbf{S}_{\hbar}-\mathbf{S}_{\hbar 1})\right\|\\ &\leq \Big(\frac{(\eta_1\mathbf{I}_{\mathbf{r}}+\eta_2\mathbf{I}_{\hbar})}{\mathbf{N}_{\hbar}}+\upsilon_{\hbar}\Big)\left\|\mathbf{S}_{\hbar}-\mathbf{S}_{\hbar 1}\right\| \end{aligned}$$

$$\leq \mathbb{L}_1 \left\| \mathbf{S}_{\hbar} - \mathbf{S}_{\hbar 1} \right\|, \tag{3.16}$$

where $\mathbb{L}_1 = \frac{\eta_1(\mathcal{K}_8+\eta_2\mathcal{K}_3)}{\mathcal{N}}$, $\left\|\mathbf{S}_{\hbar}\right\| = \sup_{\tau\in\Im}\left|\mathbf{S}_{\hbar}(\tau)\right| = \mathcal{K}_1$, $\left\|\mathbf{E}_{\hbar}\right\| = \sup_{\tau\in\Im}\left|\mathbf{E}_{\hbar}(\tau)\right| = \mathcal{K}_2$, $\left\|\mathbf{I}_{\hbar}\right\| = \sup_{\tau\in\Im}\left|\mathbf{I}_{\hbar}(\tau)\right| = \mathcal{K}_3$, $\left\|\mathbf{Q}_{\hbar}\right\| = \sup_{\tau\in\Im}\left|\mathbf{Q}_{\hbar}(\tau)\right| = \mathcal{K}_4$, $\left\|\mathbf{R}_{\hbar}\right\| = \sup_{\tau\in\Im}\left|\mathbf{R}_{\hbar}(\tau)\right| = \mathcal{K}_5$, $\left\|\mathbf{S}_{\mathbf{r}}\right\| = \sup_{\tau\in\Im}\left|\mathbf{S}_{\mathbf{r}}(\tau)\right| = \mathcal{K}_6$, and $\left\|\mathbf{E}_{\mathbf{r}}\right\| = \sup_{\tau\in\Im}\left|\mathbf{E}_{\mathbf{r}}(\tau)\right| = \mathcal{K}_7$, and $\left\|\mathbf{I}_{\mathbf{r}}\right\| = \sup_{\tau\in\Im}\left|\mathbf{I}_{\mathbf{r}}(\tau)\right| = \mathcal{K}_8$.

It is significant to mention that $\Omega_1(\tau, \mathbf{S}_{\hbar 1})$ admits the Lipschitz requirement involving the Lipschitz constant $\mathbb{L}_1 = \frac{\eta_1(\mathcal{K}_8+\eta_2\mathcal{K}_3)}{\mathcal{N}}$. Also, if $\mathbb{L}_1 \in [0, 1)$, then $\Omega_1(\tau, \mathbf{S}_{\hbar 1})$ is verified to be a contraction.

Accordingly, we can investigate the significance of the existence of $\mathbb{L}_{\ell}$, $\ell = 2, 3, ..., 8$ and the contraction condition for $\Omega_2(\tau, \mathbf{E}_{\hbar})$, $\Omega_3(\tau, \mathbf{I}_{\hbar})$, $\Omega_4(\tau, \mathbf{Q}_{\hbar})$, $\Omega_5(\tau, \mathbf{R}_{\hbar})$, $\Omega_6(\tau, \mathbf{S}_{\mathbf{r}})$ and $\Omega_7(\tau, \mathbf{E}_{\mathbf{r}})$ for $\mathbb{L}_{\ell} \in [0, 1)$, $\ell = 2, 3, ..., 8$.

At $\tau = \tau_{\mathbf{m}}$, $\mathbf{m} = 1, 2, ...$, presenting the recurrent form that follows from (3.14) gives

$$\begin{cases}
\mathbf{S}_{\hbar\mathbf{m}}(\tau) = \frac{1-\rho}{\mathbb{ABC}(\rho)}\Omega_1(\tau, \mathbf{S}_{\hbar\mathbf{m}-1}) + \frac{\rho}{\mathbb{ABC}(\rho)\Gamma(\rho)}\int_0^{\tau}\Omega_1(\varsigma, \mathbf{S}_{\hbar\mathbf{m}-1})(\tau-\varsigma)^{\rho-1}d\varsigma, \\
\mathbf{E}_{\hbar_{\mathbf{m}}}(\tau) = \frac{1-\rho}{\mathbb{ABC}(\rho)}\Omega_2(\tau, \mathbf{E}_{\hbar_{\mathbf{m}-1}}) + \frac{\rho}{\mathbb{ABC}(\rho)\Gamma(\rho)}\int_0^{\tau}\Omega_2(\varsigma, \mathbf{E}_{\hbar_{\mathbf{m}-1}})(\tau-\varsigma)^{\rho-1}d\varsigma, \\
\mathbf{I}_{\hbar_{\mathbf{m}}}(\tau) = \frac{1-\rho}{\mathbb{ABC}(\rho)}\Omega_3(\tau, \mathbf{I}_{\hbar_{\mathbf{m}-1}}) + \frac{\rho}{\mathbb{ABC}(\rho)\Gamma(\rho)}\int_0^{\tau}\Omega_3(\varsigma, \hbar_{m_{\mathbf{m}-1}})(\tau-\varsigma)^{\rho-1}d\varsigma, \\
\mathbf{Q}_{\hbar_{\mathbf{m}}}(\tau) = \frac{1-\rho}{\mathbb{ABC}(\rho)}\Omega_4(\tau, \mathbf{Q}_{\hbar_{\mathbf{m}-1}}) + \frac{\rho}{\mathbb{ABC}(\rho)\Gamma(\rho)}\int_0^{\tau}\Omega_4(\varsigma, \mathbf{Q}_{\hbar_{\mathbf{m}-1}})(\tau-\varsigma)^{\rho-1}d\varsigma, \\
\mathbf{R}_{\hbar_{\mathbf{m}}}(\tau) = \frac{1-\rho}{\mathbb{ABC}(\rho)}\Omega_5(\tau, \mathbf{R}_{\hbar_{\mathbf{m}-1}}) + \frac{\rho}{\mathbb{ABC}(\rho)\Gamma(\rho)}\int_0^{\tau}\Omega_5(\varsigma, \mathbf{R}_{\hbar_{\mathbf{m}-1}})(\tau-\varsigma)^{\rho-1}d\varsigma, \\
\mathbf{S}_{\mathbf{r}_{\mathbf{m}}}(\tau) = \frac{1-\rho}{\mathbb{ABC}(\rho)}\Omega_6(\tau, \mathbf{R}_{\hbar_{\mathbf{m}-1}}) + \frac{\rho}{\mathbb{ABC}(\rho)\Gamma(\rho)}\int_0^{\tau}\Omega_6(\varsigma, \mathbf{S}_{\mathbf{r}_{\mathbf{m}-1}})(\tau-\varsigma)^{\rho-1}d\varsigma, \\
\mathbf{E}_{\mathbf{r}_{\mathbf{m}}}(\tau) = \frac{1-\rho}{\mathbb{ABC}(\rho)}\Omega_7(\tau, \mathbf{E}_{\mathbf{r}_{\mathbf{m}-1}}) + \frac{\rho}{\mathbb{ABC}(\rho)\Gamma(\rho)}\int_0^{\tau}\Omega_7(\varsigma, \mathbf{E}_{\mathbf{r}_{\mathbf{m}-1}})(\tau-\varsigma)^{\rho-1}d\varsigma, \\
\mathbf{I}_{\mathbf{r}_{\mathbf{m}}}(\tau) = \frac{1-\rho}{\mathbb{ABC}(\rho)}\Omega_8(\tau, \mathbf{I}_{\mathbf{r}_{\mathbf{m}-1}}) + \frac{\rho}{\mathbb{ABC}(\rho)\Gamma(\rho)}\int_0^{\tau}\Omega_8(\varsigma, \mathbf{I}_{\mathbf{r}_{\mathbf{m}-1}})(\tau-\varsigma)^{\rho-1}d\varsigma
\end{cases} \tag{3.17}$$

in the presence of the ICs $\mathbf{S}_{\hbar}(0) = \mathbf{S}_{\hbar 0}$, $\mathbf{E}_{\hbar}(0) = \mathbf{E}_{\hbar_0}, \mathbf{I}_{\hbar}(0) = \mathbf{I}_{\hbar_0}, \mathbf{Q}_{\hbar}(0) = \mathbf{Q}_{\hbar_0}, \mathbf{R}_{\hbar}(0) = \mathbf{R}_{\hbar_0}, \mathbf{S}_{\mathbf{r}}(0) = \mathbf{S}_{\mathbf{r}_0}$, $\mathbf{E}_{\mathbf{r}}(0) = \mathbf{E}_{\mathbf{r}_0}$ *and* $\mathbf{I}_{\mathbf{r}}(0) = \mathbf{I}_{\mathbf{r}_0}$.

In (3.17), the differences of successive terms are expressed in the following terms:

$$\begin{aligned}
\Psi_{1\mathbf{m}}(\tau) &= \mathbf{S}_{\hbar\mathbf{m}}(\tau) - \mathbf{S}_{\hbar\mathbf{m}-1}(\tau) \\
&= \frac{1-\rho}{\mathbb{ABC}(\rho)}(\Omega_1(\tau, \mathbf{S}_{\hbar\mathbf{m}-1}) - \Omega_1(\tau, \mathbf{S}_{\hbar\mathbf{m}-2})) \\
&\quad + \frac{\rho}{\Gamma(\rho)\mathbb{ABC}(\rho)}\int_0^{\tau}(\Omega_1(\varsigma, \mathbf{S}_{\hbar\mathbf{m}-1}) - \Omega_1(\varsigma, \mathbf{S}_{\hbar\mathbf{m}-2}))(\tau-\varsigma)^{\rho-1}d\varsigma, \\
\Psi_{2\mathbf{m}}(\tau) &= \mathbf{E}_{\hbar_{\mathbf{m}}}(\tau) - \mathbf{E}_{\hbar_{\mathbf{m}-1}}(\tau) \\
&= \frac{1-\rho}{\mathbb{ABC}(\rho)}(\Omega_2(\tau, \mathbf{E}_{\hbar_{\mathbf{m}-1}}) - \Omega_2(\tau, \mathbf{E}_{\hbar_{\mathbf{m}-2}})) \\
&\quad + \frac{\rho}{\Gamma(\rho)\mathbb{ABC}(\rho)}\int_0^{\tau}(\Omega_2(\varsigma, \mathbf{E}_{\hbar_{\mathbf{m}-1}}) - \Omega_2(\varsigma, \mathbf{E}_{\hbar_{\mathbf{m}-2}}))(\tau-\varsigma)^{\rho-1}d\varsigma, \\
\Psi_{3\mathbf{m}}(\tau) &= \mathbf{I}_{\hbar_{\mathbf{m}}}(\tau) - \mathbf{I}_{\hbar_{\mathbf{m}-1}}(\tau) \\
&= \frac{1-\rho}{\mathbb{ABC}(\rho)}(\Omega_3(\tau, \mathbf{I}_{\hbar_{\mathbf{m}-1}}) - \Omega_3(\tau, \mathbf{I}_{\hbar_{\mathbf{m}-2}})) \\
&\quad + \frac{\rho}{\Gamma(\rho)\mathbb{ABC}(\rho)}\int_0^{\tau}(\Omega_3(\varsigma, \mathbf{I}_{\hbar_{\mathbf{m}-1}}) - \Omega_3(\varsigma, \mathbf{I}_{\hbar_{\mathbf{m}-2}}))(\tau-\varsigma)^{\rho-1}d\varsigma, \\
\Psi_{4\mathbf{m}}(\tau) &= \mathbf{Q}_{\hbar_{\mathbf{m}}}(\tau) - \mathbf{Q}_{\hbar_{\mathbf{m}-1}}(\tau)
\end{aligned}$$

$$
\begin{aligned}
&= \frac{1-\rho}{\mathbb{ABC}(\rho)}(\Omega_4(\tau, \mathbf{Q}_{\hbar_{\mathbf{m}-1}}) - \Omega_4(\tau, \mathbf{Q}_{\hbar_{\mathbf{m}-2}}))\\
&\quad + \frac{\rho}{\Gamma(\rho)\mathbb{ABC}(\rho)} \int_0^\tau (\Omega_4(\varsigma, \mathbf{Q}_{\hbar_{\mathbf{m}-1}}) - \Omega_4(\varsigma, \mathbf{Q}_{\hbar_{\mathbf{m}-2}}))(\tau-\varsigma)^{\rho-1} d\varsigma,\\
\Psi_{5\mathbf{m}}(\tau) &= \mathbf{R}_{\hbar_{\mathbf{m}}}(\tau) - \mathbf{R}_{\hbar_{\mathbf{m}-1}}(\tau)\\
&= \frac{1-\rho}{\mathbb{ABC}(\rho)}(\Omega_5(\tau, \mathbf{R}_{\hbar_{\mathbf{m}-1}}) - \Omega_5(\tau, \mathbf{R}_{\hbar_{\mathbf{m}-2}}))\\
&\quad + \frac{\rho}{\Gamma(\rho)\mathbb{ABC}(\rho)} \int_0^\tau (\Omega_5(\varsigma, \mathbf{R}_{\hbar_{\mathbf{m}-1}}) - \Omega_5(\varsigma, \mathbf{R}_{\hbar_{\mathbf{m}-2}}))(\tau-\varsigma)^{\rho-1} d\varsigma,\\
\Psi_{6\mathbf{m}}(\tau) &= \mathbf{S}_{\mathbf{r}_{\mathbf{m}}}(\tau) - \mathbf{S}_{\mathbf{r}_{\mathbf{m}-1}}(\tau)\\
&= \frac{1-\rho}{\mathbb{ABC}(\rho)}(\Omega_2(\tau, \mathbf{S}_{\mathbf{r}_{\mathbf{m}-1}}) - \Omega_6(\tau, \mathbf{S}_{\mathbf{r}_{\mathbf{m}-2}}))\\
&\quad + \frac{\rho}{\Gamma(\rho)\mathbb{ABC}(\rho)} \int_0^\tau (\Omega_6(\varsigma, \mathbf{S}_{\mathbf{r}_{\mathbf{m}-1}}) - \Omega_6(\varsigma, \mathbf{S}_{\mathbf{r}_{\mathbf{m}-2}}))(\tau-\varsigma)^{\rho-1} d\varsigma,\\
\Psi_{7\mathbf{m}}(\tau) &= \mathbf{E}_{\mathbf{r}_{\mathbf{m}}}(\tau) - \mathbf{E}_{\mathbf{r}_{\mathbf{m}-1}}(\tau)\\
&= \frac{1-\rho}{\mathbb{ABC}(\rho)}(\Omega_7(\tau, \mathbf{E}_{\mathbf{r}_{\mathbf{m}-1}}) - \Omega_7(\tau, \mathbf{E}_{\mathbf{r}_{\mathbf{m}-2}}))\\
&\quad + \frac{\rho}{\Gamma(\rho)\mathbb{ABC}(\rho)} \int_0^\tau (\Omega_7(\varsigma, \mathbf{S}_{\mathbf{r}_{\mathbf{m}-1}}) - \Omega_7(\varsigma, \mathbf{E}_{\mathbf{r}_{\mathbf{m}-2}}))(\tau-\varsigma)^{\rho-1} d\varsigma,\\
\Psi_{8\mathbf{m}}(\tau) &= \mathbf{I}_{\mathbf{r}_{\mathbf{m}}}(\tau) - \mathbf{I}_{\mathbf{r}_{\mathbf{m}-1}}(\tau)\\
&= \frac{1-\rho}{\mathbb{ABC}(\rho)}(\Omega_8(\tau, \mathbf{I}_{\mathbf{r}_{\mathbf{m}-1}}) - \Omega_8(\tau, \mathbf{I}_{\mathbf{r}_{\mathbf{m}-2}}))\\
&\quad + \frac{\rho}{\Gamma(\rho)\mathbb{ABC}(\rho)} \int_0^\tau (\Omega_8(\varsigma, \mathbf{I}_{\mathbf{r}_{\mathbf{m}-1}}) - \Omega_8(\varsigma, \mathbf{I}_{\mathbf{r}_{\mathbf{m}-2}}))(\tau-\varsigma)^{\rho-1} d\varsigma. \qquad (3.18)
\end{aligned}
$$

Applying the norm to the specified framework (3.18), we have

$$
\begin{aligned}
\left\|\Psi_{1\mathbf{m}}(\tau)\right\| &= \left\|\mathbf{S}_{\hbar\mathbf{m}}(\tau) - \mathbf{S}_{\hbar\mathbf{m}-1}(\tau)\right\|\\
&= \frac{1-\rho}{\mathbb{ABC}(\rho)}\left\|\Omega_1(\tau, \mathbf{S}_{\hbar\mathbf{m}-1}) - \Omega_1(\tau, \mathbf{S}_{\hbar\mathbf{m}-2})\right\|\\
&\quad + \frac{\rho}{\Gamma(\rho)\mathbb{ABC}(\rho)} \int_0^\tau \left\|\Omega_1(\varsigma, \mathbf{S}_{\hbar\mathbf{m}-1}) - \Omega_1(\varsigma, \mathbf{S}_{\hbar\mathbf{m}-2})\right\|(\tau-\varsigma)^{\rho-1} d\varsigma,\\
\left\|\Psi_{2\mathbf{m}}(\tau)\right\| &= \left\|\mathbf{E}_{\hbar_{\mathbf{m}}}(\tau) - \mathbf{E}_{\hbar_{\mathbf{m}-1}}(\tau)\right\|\\
&= \frac{1-\rho}{\mathbb{ABC}(\rho)}\left\|\Omega_2(\tau, \mathbf{E}_{\hbar_{\mathbf{m}-1}}) - \Omega_2(\tau, \mathbf{E}_{\hbar_{\mathbf{m}-2}})\right\|\\
&\quad + \frac{\rho}{\Gamma(\rho)\mathbb{ABC}(\rho)} \int_0^\tau \left\|\Omega_2(\varsigma, \mathbf{E}_{\hbar_{\mathbf{m}-1}}) - \Omega_2(\varsigma, \mathbf{E}_{\hbar_{\mathbf{m}-2}})\right\|(\tau-\varsigma)^{\rho-1} d\varsigma,\\
\left\|\Psi_{3\mathbf{m}}(\tau)\right\| &= \left\|\mathbf{I}_{\hbar_{\mathbf{m}}}(\tau) - \mathbf{I}_{\hbar_{\mathbf{m}-1}}(\tau)\right\|\\
&= \frac{1-\rho}{\mathbb{ABC}(\rho)}\left\|\Omega_3(\tau, \mathbf{I}_{\hbar_{\mathbf{m}-1}}) - \Omega_3(\tau, \mathbf{I}_{\hbar_{\mathbf{m}-2}})\right\|\\
&\quad + \frac{\rho}{\Gamma(\rho)\mathbb{ABC}(\rho)} \int_0^\tau \left\|\Omega_3(\varsigma, \mathbf{I}_{\hbar_{\mathbf{m}-1}}) - \Omega_3(\varsigma, \mathbf{I}_{\hbar_{\mathbf{m}-2}})\right\|(\tau-\varsigma)^{\rho-1} d\varsigma,\\
\left\|\Psi_{4\mathbf{m}}(\tau)\right\| &= \left\|\mathbf{Q}_{\hbar_{\mathbf{m}}}(\tau) - \mathbf{Q}_{\hbar_{\mathbf{m}-1}}(\tau)\right\|
\end{aligned}
$$

$$
\begin{aligned}
&= \frac{1-\rho}{\mathbb{ABC}(\rho)}\left\|\Omega_4(\tau,\mathbf{Q}_{\hbar_{\mathbf{m}-1}})-\Omega_4(\tau,\mathbf{Q}_{\hbar_{\mathbf{m}-2}})\right\| \\
&\quad+\frac{\rho}{\Gamma(\rho)\mathbb{ABC}(\rho)}\int_0^\tau\left\|\Omega_4(\varsigma,\mathbf{Q}_{\hbar_{\mathbf{m}-1}})-\Omega_4(\varsigma,\mathbf{Q}_{\hbar_{\mathbf{m}-2}})\right\|(\tau-\varsigma)^{\rho-1}d\varsigma,\\
\left\|\Psi_{5\mathbf{m}}(\tau)\right\| &= \left\|\mathbf{R}_{\hbar_{\mathbf{m}}}(\tau)-\mathbf{R}_{\hbar_{\mathbf{m}-1}}(\tau)\right\| \\
&= \frac{1-\rho}{\mathbb{ABC}(\rho)}\left\|\Omega_5(\tau,\mathbf{R}_{\hbar_{\mathbf{m}-1}})-\Omega_5(\tau,\mathbf{R}_{\hbar_{\mathbf{m}-2}})\right\| \\
&\quad+\frac{\rho}{\Gamma(\rho)\mathbb{ABC}(\rho)}\int_0^\tau\left\|\Omega_5(\varsigma,\mathbf{R}_{\hbar_{\mathbf{m}-1}})-\Omega_5(\varsigma,\mathbf{R}_{\hbar_{\mathbf{m}-2}})\right\|(\tau-\varsigma)^{\rho-1}d\varsigma,\\
\left\|\Psi_{6\mathbf{m}}(\tau)\right\| &= \left\|\mathbf{S}_{\mathbf{r}_{\mathbf{m}}}(\tau)-\mathbf{S}_{\mathbf{r}_{\mathbf{m}-1}}(\tau)\right\| \\
&= \frac{1-\rho}{\mathbb{ABC}(\rho)}\left\|\Omega_6(\tau,\mathbf{S}_{\mathbf{r}_{\mathbf{m}-1}})-\Omega_6(\tau,\mathbf{S}_{\mathbf{r}_{\mathbf{m}-2}})\right\| \\
&\quad+\frac{\rho}{\Gamma(\rho)\mathbb{ABC}(\rho)}\int_0^\tau\left\|\Omega_6(\varsigma,\mathbf{S}_{\mathbf{r}_{\mathbf{m}-1}})-\Omega_6(\varsigma,\mathbf{S}_{\mathbf{r}_{\mathbf{m}-2}})\right\|(\tau-\varsigma)^{\rho-1}d\varsigma,\\
\left\|\Psi_{7\mathbf{m}}(\tau)\right\| &= \left\|\mathbf{E}_{\mathbf{r}_{\mathbf{m}}}(\tau)-\mathbf{E}_{\mathbf{r}_{\mathbf{m}-1}}(\tau)\right\| \\
&= \frac{1-\rho}{\mathbb{ABC}(\rho)}\left\|\Omega_7(\tau,\mathbf{E}_{\mathbf{r}_{\mathbf{m}-1}})-\Omega_7(\tau,\mathbf{E}_{\mathbf{r}_{\mathbf{m}-2}})\right\| \\
&\quad+\frac{\rho}{\Gamma(\rho)\mathbb{ABC}(\rho)}\int_0^\tau\left\|\Omega_7(\varsigma,\mathbf{E}_{\mathbf{r}_{\mathbf{m}-1}})-\Omega_7(\varsigma,\mathbf{E}_{\mathbf{r}_{\mathbf{m}-2}})\right\|(\tau-\varsigma)^{\rho-1}d\varsigma,\\
\left\|\Psi_{8\mathbf{m}}(\tau)\right\| &= \left\|\mathbf{I}_{\mathbf{r}_{\mathbf{m}}}(\tau)-\mathbf{I}_{\mathbf{r}_{\mathbf{m}-1}}(\tau)\right\| \\
&= \frac{1-\rho}{\mathbb{ABC}(\rho)}\left\|\Omega_8(\tau,\mathbf{I}_{\mathbf{r}_{\mathbf{m}-1}})-\Omega_8(\tau,\mathbf{I}_{\mathbf{r}_{\mathbf{m}-2}})\right\| \\
&\quad+\frac{\rho}{\Gamma(\rho)\mathbb{ABC}(\rho)}\int_0^\tau\left\|\Omega_8(\varsigma,\mathbf{I}_{\mathbf{r}_{\mathbf{m}-1}})-\Omega_8(\varsigma,\mathbf{I}_{\mathbf{r}_{\mathbf{m}-2}})\right\|(\tau-\varsigma)^{\rho-1}d\varsigma. \qquad (3.19)
\end{aligned}
$$

Furthermore, the first equation in (3.19) can be converted to the following characterizations:

$$
\begin{aligned}
\left\|\Psi_{1\mathbf{m}}(\tau)\right\| &= \left\|\mathbf{S}_{\hbar\mathbf{m}}(\tau)-\mathbf{S}_{\hbar\mathbf{m}-1}(\tau)\right\| \\
&= \frac{1-\rho}{\mathbb{ABC}(\rho)}\left\|\Omega_1(\tau,\mathbf{S}_{\hbar\mathbf{m}-1})-\Omega_1(\tau,\mathbf{S}_{\hbar\mathbf{m}-2})\right\| \\
&\quad+\frac{\rho}{\Gamma(\rho)\mathbb{ABC}(\rho)}\int_0^\tau\left\|\Omega_1(\varsigma,\mathbf{S}_{\hbar\mathbf{m}-1})-\Omega_1(\varsigma,\mathbf{S}_{\hbar\mathbf{m}-2})\right\|(\tau-\varsigma)^{\rho-1}d\varsigma \\
&\le \mathbb{L}_1\frac{1-\rho}{\mathbb{ABC}(\rho)}\left\|\mathbf{S}_{\hbar\mathbf{m}-1}-\mathbf{S}_{\hbar\mathbf{m}-2}\right\|+\frac{\rho\mathbb{L}_1}{\Gamma(\rho)\mathbb{ABC}(\rho)}\int_0^\tau\left\|\mathbf{S}_{\hbar\mathbf{m}-1}-\mathbf{S}_{\hbar\mathbf{m}-2}\right\|(\tau-\varsigma)^{\rho-1}d\varsigma \\
&\le \mathbb{L}_1\left\|\Psi_{1(\mathbf{m}-1)}(\tau)\right\|\left|\frac{1-\rho}{\mathbb{ABC}(\rho)}+\frac{\tau^\rho}{\mathbb{ABC}(\rho)}\right|.
\end{aligned}
$$

Ultimately, we have

$$
\left\|\Psi_{1\mathbf{m}}(\tau)\right\| \le \mathbb{L}_1\left\|\Psi_{1(\mathbf{m}-1)}(\tau)\right\|\left|\frac{1-\rho}{\mathbb{ABC}(\rho)}+\frac{\tau^\rho}{\mathbb{ABC}(\rho)}\right|. \qquad (3.20)
$$

By a similar argument, the following terms of (3.19) can be computed as

$$
\left\|\Psi_{2\mathbf{m}}(\tau)\right\| \le \mathbb{L}_2\left\|\Psi_{2(\mathbf{m}-1)}(\tau)\right\|\left|\frac{1-\rho}{\mathbb{ABC}(\rho)}+\frac{\tau^\rho}{\mathbb{ABC}(\rho)}\right|,
$$

$$\begin{aligned}
\left\|\Psi_{3\mathbf{m}}(\tau)\right\| &\leq \mathbb{L}_3\left\|\Psi_{3(\mathbf{m}-1)}(\tau)\right\|\left|\frac{1-\rho}{\mathbb{ABC}(\rho)}+\frac{\tau^{\rho}}{\mathbb{ABC}(\rho)}\right|,\\
\left\|\Psi_{4\mathbf{m}}(\tau)\right\| &\leq \mathbb{L}_4\left\|\Psi_{4(\mathbf{m}-1)}(\tau)\right\|\left|\frac{1-\rho}{\mathbb{ABC}(\rho)}+\frac{\tau^{\rho}}{\mathbb{ABC}(\rho)}\right|,\\
\left\|\Psi_{5\mathbf{m}}(\tau)\right\| &\leq \mathbb{L}_5\left\|\Psi_{5(\mathbf{m}-1)}(\tau)\right\|\left|\frac{1-\rho}{\mathbb{ABC}(\rho)}+\frac{\tau^{\rho}}{\mathbb{ABC}(\rho)}\right|,\\
\left\|\Psi_{6\mathbf{m}}(\tau)\right\| &\leq \mathbb{L}_6\left\|\Psi_{6(\mathbf{m}-1)}(\tau)\right\|\left|\frac{1-\rho}{\mathbb{ABC}(\rho)}+\frac{\tau^{\rho}}{\mathbb{ABC}(\rho)}\right|,\\
\left\|\Psi_{7\mathbf{m}}(\tau)\right\| &\leq \mathbb{L}_7\left\|\Psi_{7(\mathbf{m}-1)}(\tau)\right\|\left|\frac{1-\rho}{\mathbb{ABC}(\rho)}+\frac{\tau^{\rho}}{\mathbb{ABC}(\rho)}\right|,\\
\left\|\Psi_{8\mathbf{m}}(\tau)\right\| &\leq \mathbb{L}_8\left\|\Psi_{8(\mathbf{m}-1)}(\tau)\right\|\left|\frac{1-\rho}{\mathbb{ABC}(\rho)}+\frac{\tau^{\rho}}{\mathbb{ABC}(\rho)}\right|.
\end{aligned} \tag{3.21}$$

Theorem 3.3. *There is a fractional $\mathbb{MPX}$ model defined in* (3.12) *that has a solution if $\mathcal{U}_0$ admits the variant*

$$\left(\frac{1-\rho}{\mathbb{ABC}(\rho)}+\frac{\mathcal{U}_0^{\rho}}{\mathbb{ABC}(\rho)\Gamma(\rho)}\right)\mathbb{L}_{\ell}<1,\quad \ell=1,2,...,8. \tag{3.22}$$

Proof. Utilizing the hypothesis stated in (3.20) and (3.23), one obtains

$$\begin{aligned}
\left\|\Psi_{1\mathbf{m}}(\tau)\right\| &\leq \left\|\mathbf{S}_{\hbar}(0)\right\|\left\{\mathbb{L}_1\left(\frac{1-\rho}{\mathbb{ABC}(\rho)}+\frac{\tau^{\rho}}{\mathbb{ABC}(\rho)}\right)\right\}^{\mathbf{m}},\\
\left\|\Psi_{2\mathbf{m}}(\tau)\right\| &\leq \left\|\mathbf{E}_{\hbar}(0)\right\|\left\{\mathbb{L}_2\left(\frac{1-\rho}{\mathbb{ABC}(\rho)}+\frac{\tau^{\rho}}{\mathbb{ABC}(\rho)}\right)\right\}^{\mathbf{m}},\\
\left\|\Psi_{3\mathbf{m}}(\tau)\right\| &\leq \left\|\mathbf{I}_{\hbar}(0)\right\|\left\{\mathbb{L}_3\left(\frac{1-\rho}{\mathbb{ABC}(\rho)}+\frac{\tau^{\rho}}{\mathbb{ABC}(\rho)}\right)\right\}^{\mathbf{m}},\\
\left\|\Psi_{4\mathbf{m}}(\tau)\right\| &\leq \left\|\mathbf{Q}_{\hbar}(0)\right\|\left\{\mathbb{L}_4\left(\frac{1-\rho}{\mathbb{ABC}(\rho)}+\frac{\tau^{\rho}}{\mathbb{ABC}(\rho)}\right)\right\}^{\mathbf{m}},\\
\left\|\Psi_{5\mathbf{m}}(\tau)\right\| &\leq \left\|\mathbf{R}_{\hbar}(0)\right\|\left\{\mathbb{L}_5\left(\frac{1-\rho}{\mathbb{ABC}(\rho)}+\frac{\tau^{\rho}}{\mathbb{ABC}(\rho)}\right)\right\}^{\mathbf{m}},\\
\left\|\Psi_{6\mathbf{m}}(\tau)\right\| &\leq \left\|\mathbf{S}_{\mathbf{r}}(0)\right\|\left\{\mathbb{L}_6\left(\frac{1-\rho}{\mathbb{ABC}(\rho)}+\frac{\tau^{\rho}}{\mathbb{ABC}(\rho)}\right)\right\}^{\mathbf{m}},\\
\left\|\Psi_{7\mathbf{m}}(\tau)\right\| &\leq \left\|\mathbf{E}_{\mathbf{r}}(0)\right\|\left\{\mathbb{L}_7\left(\frac{1-\rho}{\mathbb{ABC}(\rho)}+\frac{\tau^{\rho}}{\mathbb{ABC}(\rho)}\right)\right\}^{\mathbf{m}},\\
\left\|\Psi_{8\mathbf{m}}(\tau)\right\| &\leq \left\|\mathbf{I}_{\mathbf{r}}(0)\right\|\left\{\mathbb{L}_8\left(\frac{1-\rho}{\mathbb{ABC}(\rho)}+\frac{\tau^{\rho}}{\mathbb{ABC}(\rho)}\right)\right\}^{\mathbf{m}}.
\end{aligned} \tag{3.23}$$

Theorem 3.2 verifies the validity of the solution (the existence of a $\tilde{f_p}$) and and which shows that the mappings $\mathbf{S}_{\hbar}(\tau)$, $\mathbf{E}_{\hbar}(\tau)$, $\mathbf{I}_{\hbar}(\tau)$, $\mathbf{Q}_{\hbar}(\tau)$, $\mathbf{R}_{\hbar}(\tau)$, $\mathbf{S}_{\mathbf{r}}(\tau)$ and $\mathbf{E}_{\mathbf{r}}(\tau)$, are solution of the model (3.12).

Let us commence by identifying which criteria are fulfilled:

$$\begin{cases} \mathbf{S}_{\hbar}(\tau) - \mathbf{S}_{\hbar}(0) = \mathbf{S}_{\hbar_{\mathbf{m}}} - \tilde{B_{1\mathbf{m}}}(\tau), \\ \mathbf{E}_{\hbar}(\tau) - \mathbf{E}_{\hbar}(0) = \mathbf{E}_{\hbar_{\mathbf{m}}} - \tilde{B_{2\mathbf{m}}}(\tau), \\ \mathbf{I}_{\hbar}(\tau) - \mathbf{I}_{\hbar}(0) = \mathbf{I}_{\hbar_{\mathbf{m}}} - \tilde{B_{3\mathbf{m}}}(\tau), \\ \mathbf{Q}_{\hbar}(\tau) - \mathbf{Q}_{\hbar}(0) = \mathbf{Q}_{\hbar_{\mathbf{m}}} - \tilde{B_{4\mathbf{m}}}(\tau), \\ \mathbf{R}_{\hbar}(\tau) - \mathbf{R}_{\hbar}(0) = \mathbf{R}_{\hbar_{\mathbf{m}}} - \tilde{B_{5\mathbf{m}}}(\tau), \\ \mathbf{S}_{\mathbf{r}}(\tau) - \mathbf{S}_{\mathbf{r}}(0) = \mathbf{S}_{\mathbf{r}_{\mathbf{m}}} - \tilde{B_{6\mathbf{m}}}(\tau), \\ \mathbf{E}_{\mathbf{r}}(\tau) - \mathbf{E}_{\mathbf{r}}(0) = \mathbf{E}_{\mathbf{r}_{\mathbf{m}}} - \tilde{B_{7\mathbf{m}}}(\tau), \\ \mathbf{I}_{\mathbf{r}}(\tau) - \mathbf{I}_{\mathbf{r}}(0) = \mathbf{I}_{\mathbf{r}_{\mathbf{m}}} - \tilde{B_{8\mathbf{m}}}(\tau). \end{cases}$$

By making the use of (3.24), we have

$$\begin{aligned} \left\|B_{1\mathbf{m}}(\tau)\right\| \quad &\leq \frac{1-\rho}{\mathbb{ABC}(\rho)}\left\|\Omega_1(\tau, \mathbf{S}_{\hbar\mathbf{m}}) - \Omega_1(\tau, \mathbf{S}_{\hbar\mathbf{m}-1})\right\| \\ &\quad + \frac{\rho}{\Gamma(\rho)\mathbb{ABC}(\rho)}\int_0^{\tau}\left\|\Omega_1(\varsigma, \mathbf{S}_{\hbar\mathbf{m}}) - \Omega_1(\varsigma, \mathbf{S}_{\hbar\mathbf{m}-1})\right\|(\tau-\varsigma)^{\rho-1}d\varsigma \\ &\leq \mathbb{L}_1\frac{1-\rho}{\mathbb{ABC}(\rho)}\left\|\mathbf{S}_{\hbar\mathbf{m}} - \mathbf{S}_{\hbar\mathbf{m}-1}\right\| + \frac{\rho^{\mathbf{m}}\mathbb{L}_1}{\Gamma(\rho)\mathbb{ABC}(\rho)}\left\|\mathbf{S}_{\hbar\mathbf{m}} - \mathbf{S}_{\hbar\mathbf{m}-1}\right\|. \end{aligned}$$

Recursively conducting the procedure yields

$$\left\|B_{1\mathbf{m}}(\tau)\right\| \leq \mathbb{L}_1^{\mathbf{m}}\left\{\frac{1-\rho}{\mathbb{ABC}(\rho)} + \mathbb{L}_1^{\mathbf{m}}\frac{\tau^{\rho}}{\Gamma(\rho)\mathbb{ABC}(\rho)}\right\}^{\mathbf{m}+1}\left\|\mathbf{S}_{\hbar\mathbf{m}} - \mathbf{S}_{\hbar\mathbf{m}-1}\right\|^{\mathbf{m}}.$$

Then, $\tau = \mathcal{U}_0^{\rho}$ generates

$$\left\|B_{1\mathbf{m}}(\tau)\right\| \leq \mathbb{L}_1^{\mathbf{m}}\left\{\frac{1-\rho}{\mathbb{ABC}(\rho)} + \frac{\tau^{\rho}}{\Gamma(\rho)\mathbb{ABC}(\rho)}\right\}^{\mathbf{m}+1}\left\|\mathbf{S}_{\hbar\mathbf{m}} - \mathbf{S}_{\hbar\mathbf{m}-1}\right\|^{\mathbf{m}}. \tag{3.24}$$

This is because

$$\left\|B_{1\mathbf{m}}(\tau)\right\| \mapsto 0.$$

Let us apply the following limit to (3.24) as $\mathbf{m} \mapsto \infty$. Obviously, we have that $\left\|B_{1\mathbf{m}}(\tau)\right\| \mapsto 0$ for $\left(\frac{1-\rho}{\mathbb{ABC}(\rho)} + \frac{\tau^{\rho}}{\Gamma(\rho)\mathbb{ABC}(\rho)}\right)\mathbb{L}_1 < 1$.

In an analogous manner, we can obtain $\left\|B_{\ell\mathbf{m}}(\tau)\right\| \mapsto 0,\ for\ \ell = 2, 3, ..., 7$; then,

$\left(\frac{1-\rho}{\mathbb{ABC}(\rho)} + \frac{\tau^{\rho}}{\Gamma(\rho)\mathbb{ABC}(\rho)}\right)\mathbb{L}_{\ell} < 1,\ \ \ell = 1, 2, ..., 8.$

This gives the immediate consequence.

Furthermore, the Banach $\tilde{f_p}$ assumptions assure the existence of the system solution for (3.12) by Theorem 3.2 and Theorem 3.3. Theorem 3.4 confirms the system's uniqueness.

Theorem 3.4. *A fractional* $\mathbb{MPX}$ *system* (3.12) *has unique solution if*

$$\Big(\frac{1-\rho}{\mathbb{ABC}(\rho)}+\frac{\tau^{\rho}}{\Gamma(\rho)\mathbb{ABC}(\rho)}\Big)\mathbb{L}_{\ell}<1,\ \ \ell=1,2,...,8.$$

Proof. Suppose that $\mathbf{S}_{\hbar 1},\ \mathbf{E}_{\hbar_1},\ \mathbf{I}_{\hbar_1},\ \mathbf{Q}_{\hbar_1},\ \mathbf{R}_{\hbar_1},\ \mathbf{S}_{\mathbf{r}_1},\ \mathbf{E}_{\mathbf{r}_1}$ and $\mathbf{I}_{\mathbf{r}}$ are another solution to the fractional $\mathbb{MPX}$ system (3.12). Then

$$\mathbf{S}(\tau)-\mathbf{S}_1(\tau)=\frac{1-\rho}{\mathbb{ABC}(\rho)}(\Omega_1(\tau,\mathbf{S}_{\hbar})-\Omega_1(\tau,\mathbf{S}_{\hbar 1}))+\frac{\rho}{\mathbb{ABC}(\rho)\Gamma(\rho)}\int_0^{\tau}(\Omega_1(\varsigma,\mathbf{S}_{\hbar})-\Omega_1(\varsigma,\mathbf{S}_{\hbar 1}))(\tau-\varsigma)^{\rho-1}d\varsigma.$$

Considering the norm to the above identity, gives

$$\big\|\mathbf{S}(\tau)-\mathbf{S}_1(\tau)\big\|\leq\frac{1-\rho}{\mathbb{ABC}(\rho)}\big\|\mathbf{S}_{\hbar}-\mathbf{S}_{\hbar 1}\big\|\mathbb{L}_1+\frac{\tau^{\rho}}{\mathbb{ABC}(\rho)\Gamma(\rho)}\big\|\mathbf{S}_{\hbar}-\mathbf{S}_{\hbar 1}\big\|.$$

Since $\Big(1-\Big(\frac{1-\rho}{\mathbb{ABC}(\rho)}+\frac{\tau^{\rho}}{\Gamma(\rho)\mathbb{ABC}(\rho)}\Big)\mathbb{L}_1\Big)>0$, we acquire $\big\|\mathbf{S}_{\hbar}-\mathbf{S}_{\hbar 1}\big\|=0$. Finally, we have $\mathbf{S}_{\hbar}=\mathbf{S}_{\hbar_1}$. by the same argument, we can verify that $\mathbf{E}_{\hbar}=\mathbf{I}_{p_1},\ \mathbf{I}_{\hbar}=\mathbf{I}_{\mathbf{r}},\ \mathbf{Q}_{\hbar}=\mathbf{I}_{p\mathbf{r}},\ \mathbf{R}_{\hbar}=\mathbf{R}_{p_1},\ \mathbf{S}_{\mathbf{r}}=\mathbf{R}_{\mathbf{r}}$ and $\mathbf{E}_{\mathbf{r}}=\mathbf{R}_{p\mathbf{r}}$. This yields the immediate consequence.

3.9. Numerical scheme of $\mathbb{MPX}$ *model*

In this part, we implement the Toufik–Atangana [44] method to produce a comprehensive formulation for the framework (3.12).

When we investigate the first factor of (3.12), we obtain

$$\begin{cases}{}_0^{ABC}\mathbf{D}_{\tau}^{\rho}\mathbf{S}_{\hbar}(\tau)=\Theta_1(\tau,\mathbf{S}_{\hbar}(\tau)),\\ \mathbf{S}_{\hbar}(0)=\mathbf{S}_{\hbar 0}.\end{cases}\tag{3.25}$$

Analyzing (3.16), ones can estimate for (3.25) in the formulation stated in (3.26):

$$\mathbf{S}_{\hbar}(\tau)=\mathbf{S}_{\hbar}(0)+\frac{1-\rho}{\mathbb{ABC}(\rho)}\Theta_1(\tau,\mathbf{S}_{\hbar}(\tau))+\frac{\rho}{\mathbb{ABC}(\rho)\Gamma(\rho)}\int_0^{\tau}\Theta_1(\varsigma,\mathbf{S}_{\hbar}(\varsigma))(\tau-\varsigma)^{\rho-1}d\varsigma.\tag{3.26}$$

Considering Lagrange's interpolating polynomial approach on $[\tau_{\mathbf{q}},\tau_{\mathbf{q}+1}]$, gives

$$\begin{aligned}\mathbf{S}_{\hbar\mathbf{q}}\ \ \approx\ &\frac{1}{h_1}\Big[(\mathbf{w}-\tau_{\mathbf{q}-1})\Theta_1(\tau_{\mathbf{q}},\mathbf{S}_{\hbar}(\tau_{\mathbf{q}}),\mathbf{E}_{\hbar}(\tau_{\mathbf{q}}),\mathbf{I}_{\hbar}(\tau_{\mathbf{q}}),\mathbf{Q}_{\hbar}(\tau_{\mathbf{q}}),\mathbf{R}_{\hbar}(\tau_{\mathbf{q}}),\mathbf{S}_{\mathbf{r}}(\tau_{\mathbf{q}}),\mathbf{E}_{\mathbf{r}}(\tau_{\mathbf{q}}),\mathbf{I}_{\mathbf{r}}(\tau_{\mathbf{q}}))\\ &-(\mathbf{w}-\tau_{\mathbf{q}})\Theta_1(\tau_{\mathbf{q}-1},\mathbf{S}_{\hbar}(\tau_{\mathbf{q}-1}),\mathbf{E}_{\hbar}(\tau_{\mathbf{q}-1}),\mathbf{I}_{\hbar}(\tau_{\mathbf{q}-1}),\mathbf{Q}_{\hbar}(\tau_{\mathbf{q}-1}),\mathbf{R}_{\hbar}(\tau_{\mathbf{q}-1}),\mathbf{S}_{\mathbf{r}}(\tau_{\mathbf{q}-1}),\mathbf{E}_{\mathbf{r}}(\tau_{\mathbf{q}-1}),\mathbf{E}_{\mathbf{r}}(\tau_{\mathbf{q}-1}))\Big],\end{aligned}\tag{3.27}$$

where $h_1=\tau_{\mathbf{q}}-\tau_{\mathbf{q}-1}$.

Substituting (3.27) into (3.26), one can obtain

$$\mathbf{S}_{\hbar}(\tau_{\mathbf{m}+1})\ \ =\mathbf{S}_{\hbar}(0)+\frac{1-\rho}{\mathbb{ABC}(\rho)}\Theta_1(\tau_{\mathbf{q}},\mathbf{S}_{\hbar}(\tau_{\mathbf{q}}),\mathbf{E}_{\hbar}(\tau_{\mathbf{q}}),\mathbf{I}_{\hbar}(\tau_{\mathbf{q}}),\mathbf{Q}_{\hbar}(\tau_{\mathbf{q}}),\mathbf{R}_{\hbar}(\tau_{\mathbf{q}}),\mathbf{S}_{\mathbf{r}}(\tau_{\mathbf{q}}),\mathbf{E}_{\mathbf{r}}(\tau_{\mathbf{q}}),\mathbf{I}_{\mathbf{r}}(\tau_{\mathbf{q}}))$$

$$+\frac{\rho}{\mathbb{ABC}(\rho)\Gamma(\rho)}\sum_{\ell=1}^{\mathbf{m}}\left\{\begin{array}{l}\frac{\Theta_1\left(\tau_\ell,\mathbf{S}_\hbar(\tau_\ell),\mathbf{E}_\hbar(\tau_\ell),\mathbf{I}_\hbar(\tau_\ell),\mathbf{Q}_\hbar(\tau_\ell),\mathbf{R}_\hbar(\tau_\ell),\mathbf{S}_\mathbf{r}(\tau_\ell),\mathbf{E}_\mathbf{r}(\tau_\ell),\mathbf{I}_\mathbf{r}(\tau_\ell)\right)}{\hbar}\\ \quad\times\int_{\tau_\ell}^{\tau_{\ell+1}}(\mathbf{w}-\tau_{\ell-1})(\tau_{\mathbf{m}+1}-\mathbf{w})^{\rho-1}d\mathbf{w}\\ \quad-\frac{\Theta_1\left(\tau_{\ell-1},\mathbf{S}_\hbar(\tau_{\ell-1}),\mathbf{E}_\hbar(\tau_{\ell-1}),\mathbf{I}_\hbar(\tau_{\ell-1}),\mathbf{Q}_\hbar(\tau_{\ell-1}),\mathbf{R}_\hbar(\tau_{\ell-1}),\mathbf{S}_\mathbf{r}(\tau_{\ell-1}),\mathbf{E}_\mathbf{r}(\tau_{\ell-1}),\mathbf{I}_\mathbf{r}(\tau_{\ell-1})\right)}{\hbar}\\ \quad\times\int_{\tau_\ell}^{\tau_{\ell+1}}(\mathbf{w}-\tau_{\ell-1})(\tau_{\mathbf{m}+1}-\mathbf{w})^{\rho-1}d\mathbf{w}\end{array}\right.$$

$$=\mathbf{S}_\hbar(0)+\frac{1-\rho}{\mathbb{ABC}(\rho)}\Theta_1(\tau_\mathbf{m},\mathbf{S}_\hbar(\tau_\mathbf{m}),\mathbf{E}_\hbar(\tau_\mathbf{m}),\mathbf{I}_\hbar(\tau_\mathbf{m}),\mathbf{Q}_\hbar(\tau_\mathbf{m}),\mathbf{R}_\hbar(\tau_\mathbf{m}),\mathbf{S}_\mathbf{r}(\tau_\mathbf{m}),\mathbf{E}_\mathbf{r}(\tau_\mathbf{m}),\mathbf{I}_\mathbf{r}(\tau_\mathbf{m}))$$

$$+\frac{\rho}{\mathbb{ABC}(\rho)\Gamma(\rho)}\sum_{\ell=1}^{\mathbf{m}}\left(\begin{array}{l}\frac{\Theta_1\left(\tau_\ell,\mathbf{S}_\hbar(\tau_\ell),\mathbf{E}_\hbar(\tau_\ell),\mathbf{I}_\hbar(\tau_\ell),\mathbf{Q}_\hbar(\tau_\ell),\mathbf{R}_\hbar(\tau_\ell),\mathbf{S}_\mathbf{r}(\tau_\ell),\mathbf{E}_\mathbf{r}(\tau_\ell),\mathbf{I}_\mathbf{r}(\tau_\ell)\right)}{h_1}\mathfrak{I}_{\ell-1}\\ \quad-\frac{\Theta_1\left(\tau_{\ell-1},\mathbf{S}_\hbar(\tau_{\ell-1}),\mathbf{E}_\hbar(\tau_{\ell-1}),\mathbf{I}_\hbar(\tau_{\ell-1}),\mathbf{Q}_\hbar(\tau_{\ell-1}),\mathbf{R}_\hbar(\tau_{\ell-1}),\mathbf{S}_\mathbf{r}(\tau_{\ell-1}),\mathbf{E}_\mathbf{r}(\tau_{\ell-1}),\mathbf{I}_\mathbf{r}(\tau_{\ell-1})\right)}{h_1}\mathfrak{I}_\ell\end{array}\right),$$

where

$$\begin{aligned}\mathfrak{I}_{\ell-1}&=\int_{\tau_\ell}^{\tau_{\ell+1}}(\mathbf{w}-\tau_{\ell-1})(\tau_{\mathbf{m}+1}-\mathbf{w})^{\rho-1}d\mathbf{w}\\&=-\frac{1}{\rho}\Big\{(\tau_{\ell+1}-\tau_{\ell-1})(\tau_{\mathbf{m}+1}-\tau_{\ell+1})^\rho-(\tau_\ell-\tau_{\ell-1})(\tau_{\mathbf{m}+1}-\tau_\ell)^\rho\Big\}\\&\quad-\frac{1}{\rho(\rho+1)}\Big\{(\tau_{\mathbf{m}+1}-\tau_{\ell+1})^{\rho+1}(\tau_{\mathbf{m}+1}-\tau_{\ell+1})^\rho-(\tau_{\mathbf{m}+1}-\tau_\ell)^{\rho+1}\Big\},\end{aligned}\tag{3.28}$$

and

$$\begin{aligned}\mathfrak{I}_{\ell}&=\int_{\tau_\ell}^{\tau_{\ell+1}}(\mathbf{w}-\tau_{\ell-1})(\tau_{\mathbf{m}+1}-\mathbf{w})^{\rho-1}d\mathbf{w}\\&=-\frac{1}{\rho}\Big\{(\tau_{\ell+1}-\tau_{\ell-1})(\tau_{\mathbf{m}+1}-\tau_{\ell+1})^\rho\Big\}\\&\quad-\frac{1}{\rho(\rho+1)}\Big\{(\tau_{\mathbf{m}+1}-\tau_{\ell+1})^{\rho+1}-(\tau_{\mathbf{m}+1}-\tau_\ell)^{\rho+1}\Big\}.\end{aligned}\tag{3.29}$$

Moreover, employing $\tau_\ell=\ell\hbar$ in (3.28) and (3.29) describes

$$\mathfrak{I}_{\ell-1}=\frac{\hbar^{\rho+1}}{\rho(\rho+1)}\Big\{(\mathbf{m}+1-\ell)^\rho(\mathbf{m}-\ell+2+\rho)-(\mathbf{m}-\ell)^\rho(\mathbf{m}-\ell+2+2\rho)\Big\}\tag{3.30}$$

and

$$\mathfrak{I}_{\ell}=\frac{\hbar^{\rho+1}}{\rho(\rho+1)}\Big\{(\mathbf{m}+1-\ell)^{\rho+1}-(\mathbf{m}-\ell)^\rho(\mathbf{m}-\ell+1+\rho)\Big\}.\tag{3.31}$$

Consequently, we can express (3.32) in the expression of (3.30) and (3.31) as follows:

$$\begin{aligned}\mathbf{S}_\hbar(\tau_{\mathbf{m}+1})&=\mathbf{S}_\hbar(\tau_0)+\frac{1-\rho}{\mathbb{ABC}(\rho)}\Theta_1(\tau_\mathbf{m},\mathbf{S}_\hbar(\tau_\mathbf{m}),\mathbf{E}_\hbar(\tau_\mathbf{m}),\mathbf{I}_\hbar(\tau_\mathbf{m}),\mathbf{Q}_\hbar(\tau_\mathbf{m}),\mathbf{R}_\hbar(\tau_\mathbf{m}),\mathbf{S}_\mathbf{r}(\tau_\mathbf{m}),\mathbf{E}_\mathbf{r}(\tau_\mathbf{m}),\mathbf{I}_\mathbf{r}(\tau_\mathbf{m}))\\&\quad+\frac{\rho}{\mathbb{ABC}(\rho)\Gamma(\rho)}\sum_{\ell=1}^{\mathbf{m}}\left(\begin{array}{l}\frac{\Theta_1\left(\tau_\ell,\mathbf{S}_\hbar(\tau_\ell),\mathbf{E}_\hbar(\tau_\ell),\mathbf{I}_\hbar(\tau_\ell),\mathbf{Q}_\hbar(\tau_\ell),\mathbf{R}_\hbar(\tau_\ell),\mathbf{S}_\mathbf{r}(\tau_\ell),\mathbf{E}_\mathbf{r}(\tau_\ell),\mathbf{I}_\mathbf{r}(\tau_\ell)\right)}{\Gamma(\rho+2)}\\ \quad\times h_1^\rho\Big\{(\mathbf{m}+1-\ell)^\rho(\mathbf{m}-\ell+2+\rho)-(\mathbf{m}-\ell)^\rho(\mathbf{m}-\ell+2+2\rho)\Big\}\\ \quad-\frac{\Theta_1\left(\tau_{\ell-1},\mathbf{S}_\hbar(\tau_{\ell-1}),\mathbf{E}_\hbar(\tau_{\ell-1}),\mathbf{I}_\hbar(\tau_{\ell-1}),\mathbf{Q}_\hbar(\tau_{\ell-1}),\mathbf{R}_\hbar(\tau_{\ell-1}),\mathbf{S}_\mathbf{r}(\tau_{\ell-1}),\mathbf{E}_\mathbf{r}(\tau_{\ell-1}),\mathbf{I}_\mathbf{r}(\tau_{\ell-1})\right)}{h_1}\\ \quad\times h_1^\rho\Big\{(\mathbf{m}+1-\ell)^\rho(\mathbf{m}-\ell+2+\rho)-(\mathbf{m}-\ell)^\rho(\mathbf{m}-\ell+2+2\rho)\Big\}\end{array}\right).\end{aligned}$$

Thus, the following are the descriptions for the rest of the model cohorts:

$$\begin{aligned}
\mathbf{E}_{\hbar}(\tau_{\mathbf{m+1}}) &= \mathbf{E}_{\hbar}(\tau_0)+\frac{1-\rho}{\mathbb{ABC}(\rho)}\Theta_2(\tau_{\mathbf{m}},\mathbf{S}_{\hbar}(\tau_{\mathbf{m}}),\mathbf{E}_{\hbar}(\tau_{\mathbf{m}}),\mathbf{I}_{\hbar}(\tau_{\mathbf{m}}),\mathbf{Q}_{\hbar}(\tau_{\mathbf{m}}),\mathbf{R}_{\hbar}(\tau_{\mathbf{m}}),\mathbf{S}_{\mathbf{r}}(\tau_{\mathbf{m}}),\mathbf{E}_{\mathbf{r}}(\tau_{\mathbf{m}}),\mathbf{I}_{\mathbf{r}}(\tau_{\mathbf{m}}))\\
&\quad+\frac{\rho}{\mathbb{ABC}(\rho)\Gamma(\rho)}\sum_{\ell=1}^{\mathbf{m}}\left(\begin{cases}\frac{\Theta_2\left(\tau_\ell,\mathbf{S}_{\hbar}(\tau_\ell),\mathbf{E}_{\hbar}(\tau_\ell),\mathbf{I}_{\hbar}(\tau_\ell),\mathbf{Q}_{\hbar}(\tau_\ell),\mathbf{R}_{\hbar}(\tau_\ell),\mathbf{S}_{\mathbf{r}}(\tau_\ell),\mathbf{E}_{\mathbf{r}}(\tau_\ell),\mathbf{I}_{\mathbf{r}}(\tau_\ell)\right)}{\Gamma(\rho+2)}\\ \quad\times h_1^{\rho}\Big\{(\mathbf{m}+1-\ell)^{\rho}(\mathbf{m}-\ell+2+\rho)-(\mathbf{m}-\ell)^{\rho}(\mathbf{m}-\ell+2+2\rho)\Big\}\\ -\frac{\Theta_2\left(\tau_{\ell-1},\mathbf{S}_{\hbar}(\tau_{\ell-1}),\mathbf{E}_{\hbar}(\tau_{\ell-1}),\mathbf{I}_{\hbar}(\tau_{\ell-1}),\mathbf{Q}_{\hbar}(\tau_{\ell-1}),\mathbf{R}_{\hbar}(\tau_{\ell-1}),\mathbf{S}_{\mathbf{r}}(\tau_{\ell-1}),\mathbf{E}_{\mathbf{r}}(\tau_{\ell-1}),\mathbf{I}_{\mathbf{r}}(\tau_{\ell-1})\right)}{h_1}\\ \quad\times h_1^{\rho}\Big\{(\mathbf{m}+1-\ell)^{\rho}(\mathbf{m}-\ell+2+\rho)-(\mathbf{m}-\ell)^{\rho}(\mathbf{m}-\ell+2+2\rho)\Big\}\end{cases}\right),\\
\mathbf{I}_{\hbar}(\tau_{\mathbf{m+1}}) &= \mathbf{I}_{\hbar}(\tau_0)+\frac{1-\rho}{\mathbb{ABC}(\rho)}\Theta_3(\tau_{\mathbf{m}},\mathbf{S}_{\hbar}(\tau_{\mathbf{m}}),\mathbf{E}_{\hbar}(\tau_{\mathbf{m}}),\mathbf{I}_{\hbar}(\tau_{\mathbf{m}}),\mathbf{Q}_{\hbar}(\tau_{\mathbf{m}}),\mathbf{R}_{\hbar}(\tau_{\mathbf{m}}),\mathbf{S}_{\mathbf{r}}(\tau_{\mathbf{m}}),\mathbf{E}_{\mathbf{r}}(\tau_{\mathbf{m}}),\mathbf{I}_{\mathbf{r}}(\tau_{\mathbf{m}}))\\
&\quad+\frac{\rho}{\mathbb{ABC}(\rho)\Gamma(\rho)}\sum_{\ell=1}^{\mathbf{m}}\left(\begin{cases}\frac{\Theta_3\left(\tau_\ell,\mathbf{S}_{\hbar}(\tau_\ell),\mathbf{E}_{\hbar}(\tau_\ell),\mathbf{I}_{\hbar}(\tau_\ell),\mathbf{Q}_{\hbar}(\tau_\ell),\mathbf{R}_{\hbar}(\tau_\ell),\mathbf{S}_{\mathbf{r}}(\tau_\ell),\mathbf{E}_{\mathbf{r}}(\tau_\ell),\mathbf{I}_{\mathbf{r}}(\tau_\ell)\right)}{\Gamma(\rho+2)}\\ \quad\times h_1^{\rho}\Big\{(\mathbf{m}+1-\ell)^{\rho}(\mathbf{m}-\ell+2+\rho)-(\mathbf{m}-\ell)^{\rho}(\mathbf{m}-\ell+2+2\rho)\Big\}\\ -\frac{\Theta_3\left(\tau_{\ell-1},\mathbf{S}_{\hbar}(\tau_{\ell-1}),\mathbf{E}_{\hbar}(\tau_{\ell-1}),\mathbf{I}_{\hbar}(\tau_{\ell-1}),\mathbf{Q}_{\hbar}(\tau_{\ell-1}),\mathbf{R}_{\hbar}(\tau_{\ell-1}),\mathbf{S}_{\mathbf{r}}(\tau_{\ell-1}),\mathbf{E}_{\mathbf{r}}(\tau_{\ell-1}),\mathbf{I}_{\mathbf{r}}(\tau_{\ell-1})\right)}{h_1}\\ \quad\times h_1^{\rho}\Big\{(\mathbf{m}+1-\ell)^{\rho}(\mathbf{m}-\ell+2+\rho)-(\mathbf{m}-\ell)^{\rho}(\mathbf{m}-\ell+2+2\rho)\Big\}\end{cases}\right),\\
\mathbf{Q}_{\hbar}(\tau_{\mathbf{m+1}}) &= \mathbf{Q}_{\hbar}(\tau_0)+\frac{1-\rho}{\mathbb{ABC}(\rho)}\Theta_4(\tau_{\mathbf{m}},\mathbf{S}_{\hbar}(\tau_{\mathbf{m}}),\mathbf{E}_{\hbar}(\tau_{\mathbf{m}}),\mathbf{I}_{\hbar}(\tau_{\mathbf{m}}),\mathbf{Q}_{\hbar}(\tau_{\mathbf{m}}),\mathbf{R}_{\hbar}(\tau_{\mathbf{m}}),\mathbf{S}_{\mathbf{r}}(\tau_{\mathbf{m}}),\mathbf{E}_{\mathbf{r}}(\tau_{\mathbf{m}}),\mathbf{I}_{\mathbf{r}}(\tau_{\mathbf{m}}))\\
&\quad+\frac{\rho}{\mathbb{ABC}(\rho)\Gamma(\rho)}\sum_{\ell=1}^{\mathbf{m}}\left(\begin{cases}\frac{\Theta_4\left(\tau_\ell,\mathbf{S}_{\hbar}(\tau_\ell),\mathbf{E}_{\hbar}(\tau_\ell),\mathbf{I}_{\hbar}(\tau_\ell),\mathbf{Q}_{\hbar}(\tau_\ell),\mathbf{R}_{\hbar}(\tau_\ell),\mathbf{S}_{\mathbf{r}}(\tau_\ell),\mathbf{E}_{\mathbf{r}}(\tau_\ell),\mathbf{I}_{\mathbf{r}}(\tau_\ell)\right)}{\Gamma(\rho+2)}\\ \quad\times h_1^{\rho}\Big\{(\mathbf{m}+1-\ell)^{\rho}(\mathbf{m}-\ell+2+\rho)-(\mathbf{m}-\ell)^{\rho}(\mathbf{m}-\ell+2+2\rho)\Big\}\\ -\frac{\Theta_4\left(\tau_{\ell-1},\mathbf{S}_{\hbar}(\tau_{\ell-1}),\mathbf{E}_{\hbar}(\tau_{\ell-1}),\mathbf{I}_{\hbar}(\tau_{\ell-1}),\mathbf{Q}_{\hbar}(\tau_{\ell-1}),\mathbf{R}_{\hbar}(\tau_{\ell-1}),\mathbf{S}_{\mathbf{r}}(\tau_{\ell-1}),\mathbf{E}_{\mathbf{r}}(\tau_{\ell-1}),\mathbf{I}_{\mathbf{r}}(\tau_{\ell-1})\right)}{h_1}\\ \quad\times h_1^{\rho}\Big\{(\mathbf{m}+1-\ell)^{\rho}(\mathbf{m}-\ell+2+\rho)-(\mathbf{m}-\ell)^{\rho}(\mathbf{m}-\ell+2+2\rho)\Big\}\end{cases}\right),\\
\mathbf{R}_{\hbar}(\tau_{\mathbf{m+1}}) &= \mathbf{R}_{\hbar}(\tau_0)+\frac{1-\rho}{\mathbb{ABC}(\rho)}\Theta_5(\tau_{\mathbf{m}},\mathbf{S}_{\hbar}(\tau_{\mathbf{m}}),\mathbf{E}_{\hbar}(\tau_{\mathbf{m}}),\mathbf{I}_{\hbar}(\tau_{\mathbf{m}}),\mathbf{Q}_{\hbar}(\tau_{\mathbf{m}}),\mathbf{R}_{\hbar}(\tau_{\mathbf{m}}),\mathbf{S}_{\mathbf{r}}(\tau_{\mathbf{m}}),\mathbf{E}_{\mathbf{r}}(\tau_{\mathbf{m}}),\mathbf{I}_{\mathbf{r}}(\tau_{\mathbf{m}}))\\
&\quad+\frac{\rho}{\mathbb{ABC}(\rho)\Gamma(\rho)}\sum_{\ell=1}^{\mathbf{m}}\left(\begin{cases}\frac{\Theta_5\left(\tau_\ell,\mathbf{S}_{\hbar}(\tau_\ell),\mathbf{E}_{\hbar}(\tau_\ell),\mathbf{I}_{\hbar}(\tau_\ell),\mathbf{Q}_{\hbar}(\tau_\ell),\mathbf{R}_{\hbar}(\tau_\ell),\mathbf{S}_{\mathbf{r}}(\tau_\ell),\mathbf{E}_{\mathbf{r}}(\tau_\ell),\mathbf{I}_{\mathbf{r}}(\tau_\ell)\right)}{\Gamma(\rho+2)}\\ \quad\times h_1^{\rho}\Big\{(\mathbf{m}+1-\ell)^{\rho}(\mathbf{m}-\ell+2+\rho)-(\mathbf{m}-\ell)^{\rho}(\mathbf{m}-\ell+2+2\rho)\Big\}\\ -\frac{\Theta_5\left(\tau_{\ell-1},\mathbf{S}_{\hbar}(\tau_{\ell-1}),\mathbf{E}_{\hbar}(\tau_{\ell-1}),\mathbf{I}_{\hbar}(\tau_{\ell-1}),\mathbf{Q}_{\hbar}(\tau_{\ell-1}),\mathbf{R}_{\hbar}(\tau_{\ell-1}),\mathbf{S}_{\mathbf{r}}(\tau_{\ell-1}),\mathbf{E}_{\mathbf{r}}(\tau_{\ell-1}),\mathbf{I}_{\mathbf{r}}(\tau_{\ell-1})\right)}{h_1}\\ \quad\times h_1^{\rho}\Big\{(\mathbf{m}+1-\ell)^{\rho}(\mathbf{m}-\ell+2+\rho)-(\mathbf{m}-\ell)^{\rho}(\mathbf{m}-\ell+2+2\rho)\Big\}\end{cases}\right),\\
\mathbf{S}_{\mathbf{r}}(\tau_{\mathbf{m+1}}) &= \mathbf{S}_{\mathbf{r}}(\tau_0)+\frac{1-\rho}{\mathbb{ABC}(\rho)}\Theta_6(\tau_{\mathbf{m}},\mathbf{S}_{\hbar}(\tau_{\mathbf{m}}),\mathbf{E}_{\hbar}(\tau_{\mathbf{m}}),\mathbf{I}_{\hbar}(\tau_{\mathbf{m}}),\mathbf{Q}_{\hbar}(\tau_{\mathbf{m}}),\mathbf{R}_{\hbar}(\tau_{\mathbf{m}}),\mathbf{S}_{\mathbf{r}}(\tau_{\mathbf{m}}),\mathbf{E}_{\mathbf{r}}(\tau_{\mathbf{m}}),\mathbf{I}_{\mathbf{r}}(\tau_{\mathbf{m}}))\\
&\quad+\frac{\rho}{\mathbb{ABC}(\rho)\Gamma(\rho)}\sum_{\ell=1}^{\mathbf{m}}\left(\begin{cases}\frac{\Theta_6\left(\tau_\ell,\mathbf{S}_{\hbar}(\tau_\ell),\mathbf{E}_{\hbar}(\tau_\ell),\mathbf{I}_{\hbar}(\tau_\ell),\mathbf{Q}_{\hbar}(\tau_\ell),\mathbf{R}_{\hbar}(\tau_\ell),\mathbf{S}_{\mathbf{r}}(\tau_\ell),\mathbf{E}_{\mathbf{r}}(\tau_\ell),\mathbf{I}_{\mathbf{r}}(\tau_\ell)\right)}{\Gamma(\rho+2)}\\ \quad\times h_1^{\rho}\Big\{(\mathbf{m}+1-\ell)^{\rho}(\mathbf{m}-\ell+2+\rho)-(\mathbf{m}-\ell)^{\rho}(\mathbf{m}-\ell+2+2\rho)\Big\}\\ -\frac{\Theta_6\left(\tau_{\ell-1},\mathbf{S}_{\hbar}(\tau_{\ell-1}),\mathbf{E}_{\hbar}(\tau_{\ell-1}),\mathbf{I}_{\hbar}(\tau_{\ell-1}),\mathbf{Q}_{\hbar}(\tau_{\ell-1}),\mathbf{R}_{\hbar}(\tau_{\ell-1}),\mathbf{S}_{\mathbf{r}}(\tau_{\ell-1}),\mathbf{E}_{\mathbf{r}}(\tau_{\ell-1}),\mathbf{I}_{\mathbf{r}}(\tau_{\ell-1})\right)}{h_1}\\ \quad\times h_1^{\rho}\Big\{(\mathbf{m}+1-\ell)^{\rho}(\mathbf{m}-\ell+2+\rho)-(\mathbf{m}-\ell)^{\rho}(\mathbf{m}-\ell+2+2\rho)\Big\}\end{cases}\right),
\end{aligned}$$

$$\mathbf{E_r}(\tau_{\mathbf{m}+1}) = \mathbf{E_r}(\tau_0) + \frac{1-\rho}{\mathbb{ABC}(\rho)}\Theta_7(\tau_{\mathbf{m}}, \mathbf{S}_{\hbar}(\tau_{\mathbf{m}}), \mathbf{E}_{\hbar}(\tau_{\mathbf{m}}), \mathbf{I}_{\hbar}(\tau_{\mathbf{m}}), \mathbf{Q}_{\hbar}(\tau_{\mathbf{m}}), \mathbf{R}_{\hbar}(\tau_{\mathbf{m}}), \mathbf{S_r}(\tau_{\mathbf{m}}), \mathbf{E_r}(\tau_{\mathbf{m}}), \mathbf{I_r}(\tau_{\mathbf{m}}))$$
$$+\frac{\rho}{\mathbb{ABC}(\rho)\Gamma(\rho)}\sum_{\ell=1}^{\mathbf{m}}\left(\begin{array}{l}\frac{\Theta_7\left(\tau_\ell,\mathbf{S}_{\hbar}(\tau_\ell),\mathbf{E}_{\hbar}(\tau_\ell),\mathbf{I}_{\hbar}(\tau_\ell),\mathbf{Q}_{\hbar}(\tau_\ell),\mathbf{R}_{\hbar}(\tau_\ell),\mathbf{S_r}(\tau_\ell),\mathbf{E_r}(\tau_\ell),\mathbf{I_r}(\tau_\ell)\right)}{\Gamma(\rho+2)}\\ \quad\times h_1^{\rho}\Big\{(\mathbf{m}+1-\ell)^{\rho}(\mathbf{m}-\ell+2+\rho)-(\mathbf{m}-\ell)^{\rho}(\mathbf{m}-\ell+2+2\rho)\Big\}\\ -\frac{\Theta_7\left(\tau_{\ell-1},\mathbf{S}_{\hbar}(\tau_{\ell-1}),\mathbf{E}_{\hbar}(\tau_{\ell-1}),\mathbf{I}_{\hbar}(\tau_{\ell-1}),\mathbf{Q}_{\hbar}(\tau_{\ell-1}),\mathbf{R}_{\hbar}(\tau_{\ell-1}),\mathbf{S_r}(\tau_{\ell-1}),\mathbf{E_r}(\tau_{\ell-1}),\mathbf{I_r}(\tau_{\ell-1})\right)}{h_1}\\ \quad\times h_1^{\rho}\Big\{(\mathbf{m}+1-\ell)^{\rho}(\mathbf{m}-\ell+2+\rho)-(\mathbf{m}-\ell)^{\rho}(\mathbf{m}-\ell+2+2\rho)\Big\}\end{array}\right).$$

$$\mathbf{I_r}(\tau_{\mathbf{m}+1}) = \mathbf{I_r}(\tau_0) + \frac{1-\rho}{\mathbb{ABC}(\rho)}\Theta_8(\tau_{\mathbf{m}}, \mathbf{S}_{\hbar}(\tau_{\mathbf{m}}), \mathbf{E}_{\hbar}(\tau_{\mathbf{m}}), \mathbf{I}_{\hbar}(\tau_{\mathbf{m}}), \mathbf{Q}_{\hbar}(\tau_{\mathbf{m}}), \mathbf{R}_{\hbar}(\tau_{\mathbf{m}}), \mathbf{S_r}(\tau_{\mathbf{m}}), \mathbf{E_r}(\tau_{\mathbf{m}}), \mathbf{I_r}(\tau_{\mathbf{m}}))$$
$$+\frac{\rho}{\mathbb{ABC}(\rho)\Gamma(\rho)}\sum_{\ell=1}^{\mathbf{m}}\left(\begin{array}{l}\frac{\Theta_8\left(\tau_\ell,\mathbf{S}_{\hbar}(\tau_\ell),\mathbf{E}_{\hbar}(\tau_\ell),\mathbf{I}_{\hbar}(\tau_\ell),\mathbf{Q}_{\hbar}(\tau_\ell),\mathbf{R}_{\hbar}(\tau_\ell),\mathbf{S_r}(\tau_\ell),\mathbf{E_r}(\tau_\ell),\mathbf{I_r}(\tau_\ell)\right)}{\Gamma(\rho+2)}\\ \quad\times h_1^{\rho}\Big\{(\mathbf{m}+1-\ell)^{\rho}(\mathbf{m}-\ell+2+\rho)-(\mathbf{m}-\ell)^{\rho}(\mathbf{m}-\ell+2+2\rho)\Big\}\\ -\frac{\Theta_8\left(\tau_{\ell-1},\mathbf{S}_{\hbar}(\tau_{\ell-1}),\mathbf{E}_{\hbar}(\tau_{\ell-1}),\mathbf{I}_{\hbar}(\tau_{\ell-1}),\mathbf{Q}_{\hbar}(\tau_{\ell-1}),\mathbf{R}_{\hbar}(\tau_{\ell-1}),\mathbf{S_r}(\tau_{\ell-1}),\mathbf{E_r}(\tau_{\ell-1}),\mathbf{I_r}(\tau_{\ell-1})\right)}{h_1}\\ \quad\times h_1^{\rho}\Big\{(\mathbf{m}+1-\ell)^{\rho}(\mathbf{m}-\ell+2+\rho)-(\mathbf{m}-\ell)^{\rho}(\mathbf{m}-\ell+2+2\rho)\Big\}\end{array}\right).$$

4. Results and discussion

Nonlinearities exist in both the integer-order and projected fractional-order systems, necessitating the application of the development of computational approaches to produce the requisite simulation model. For dynamic simulations of the mathematical formalism, a standard numerical approach from conventional calculus characterized as the Lagrange polynomial [44], has been employed; but, for fractional-order structures, recently created numerical techniques in [32, 35, 54] were implemented by utilizing the Atangana-Baleanu fractional derivative operator. Furthermore, the basic reproduction number is an important metric in patterns since it provides us with a plethora of data about the condition. We presented stability projections demonstrating the fluctuations of $\mathbb{R}_0$ by using influential factors to analyze the influence of numerous disease spreading characteristics on the basic reproductive number.

Figures 4–7 shows that $\mathbb{MPX}$ and variola infections are phylogenically connected and the smallpox vaccine is 65 % efficacious in eliminating $\mathbb{MPX}$ within the Atangana-Baleanu fractional derivative operator. Cross-reactive immune responses exist against the Orthopoxvirus genera, which means that immunized people have a considerably reduced chance of illness and fatality than uninfected people. For the purpose of clarification, the vaccine's unsatisfactory protection probability was deleted from the numerical model's formulation. Inadequate fortification, as highlighted in [55], exacerbates the challenge of proactive preventive acts, as poorer vaccine efficiency can contribute to higher vaccine penetration and indicative impacts; meanwhile, the epidemic's influence can be more difficult to ameliorate. We can deduce that diminishing the fractional-order ρ significantly decreases the occurrence of vulnerable, exposed, infectious, isolated and restored human populations as well as the rodent community.

As shown in Figures 8–11, determining the value of $\varphi_{\hbar}$ reduces virus transmission. In addition to immunization, it would be interesting to identify and evaluate potential preventive interventions that could have a discernible impact on $\mathbb{MPX}$ propagation. For example, reducing animal-to-human

interaction and starting an awareness program about the consequences of consuming unprocessed meat, which appears to be the primary cause of squirrel-to-human [56] dissemination, would drastically reduce the animal-to-human propagation incidence. It may result in a high operating cost (for example, a reduction in meat availability), but it does not necessitate the costly or poorly functioning healthcare systems required for vaccination, providing the public with a commonly approachable prophylactic strategy. Such an amendment's mathematical analysis would grow more complicated. The basic idea may be similar to that of [57], the authors of which investigated cholera preventative conditions in which people could be vaccinated or consume dangerously toxic water. Figures 8–11 show how dropping the ρ from 1 deflects the susceptible human incident $\mathbf{S}_{\hbar}$ curves, resulting in a considerable mitigation in the number of occurrences in the cohorts.

The level of interaction involving the rodent community has a significant effect on the $\mathbb{MPX}$ spread, as shown in Figures 12–15. We included a cohort $\mathbf{Q}_{\hbar}$ in the model, which contains the separated portion of infectious individuals. We demonstrated how the contaminated community would respond in the context of specific treatments by using numerical modeling. Furthermore, the real data [43] included with the fractional-order, which predicts that real data is in strong harmony the fractional-order one.

In a nutshell, Figures 16–19 depicts a cumulative comparative evaluation of both classical and suggested fractional-order modelling techniques with preventive measures and non-preventive measures, showing that several of the observations from the Atangana–Baleanu operator are pretty close to the factual arguments for about 8 weeks, indicating that the suggested fractional-order derivative operator has the best effectiveness proportion.

Hence, we conclude that Atangana-Baleanu fractional-order modeling in the Caputo context is still a useful approach for gaining a better grasp of how $\mathbb{MPX}$ works in different situations. Epidemiologic modelling and fractional analysis have a broad array of applications. We expect that the simulations can be used as a prognostic approach to precisely comprehend the transmission of $\mathbb{MPX}$ as more occurrences of the virus are documented in the human population.

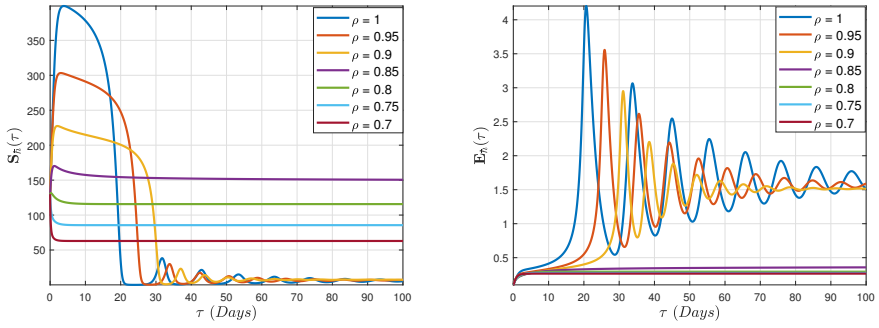

(a) **(b)**

Figure 4. Graphical illustration of the susceptible group $\mathbf{S}_{\hbar}(\tau)$ and exposed individuals $\mathbf{E}_{\hbar}(\tau)$ for the human population when δ_2 decreases considering multiple fractional orders $\rho \in [0, 1]$.

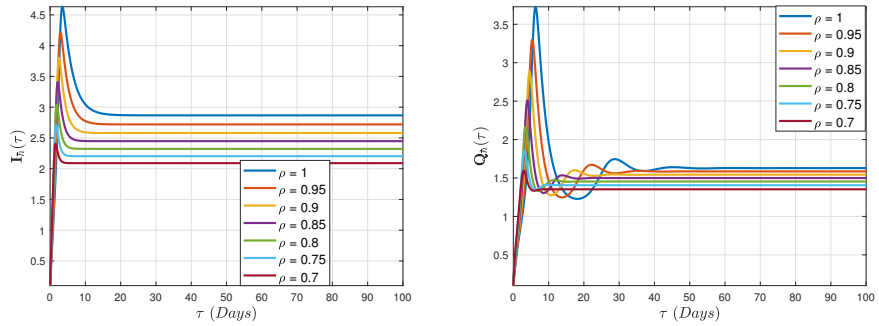

(a) **(b)**

Figure 5. Graphical illustration of the infectious group $\mathbf{I}_{\hbar}(\tau)$ and isolated individuals $\mathbf{Q}_{\hbar}(\tau)$ for the human population when δ_2 decreases considering multiple fractional orders $\rho \in [0, 1]$.

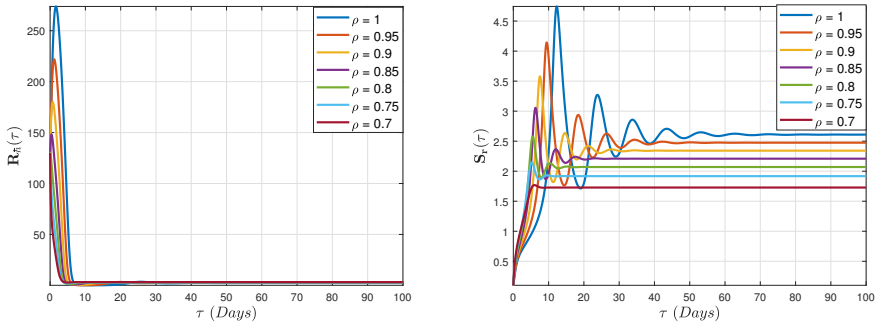

(a) **(b)**

Figure 6. Graphical illustration of the recovered human group $\mathbf{R}_{\hbar}(\tau)$ and exposed individuals $\mathbf{E}_{\mathbf{r}}(\tau)$ for the rodent population when δ_2 decreases considering multiple fractional orders $\rho \in [0, 1]$.

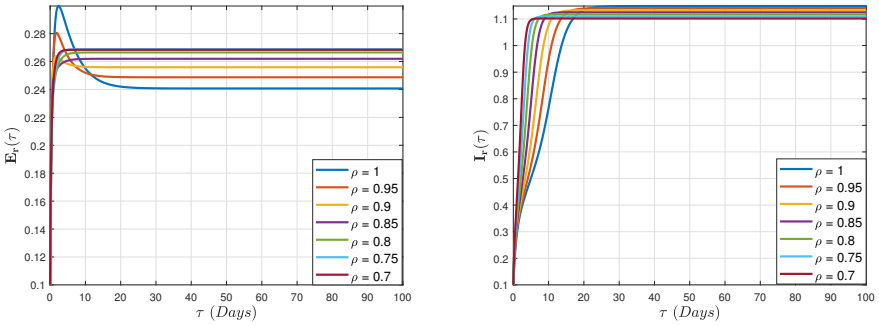

(a) **(b)**

Figure 7. Graphical illustration of the exposed group $\mathbf{E}_{\mathbf{r}}(\tau)$ and infectious individuals $\mathbf{I}_{\mathbf{r}}(\tau)$ for the rodent population when δ_2 decreases considering multiple fractional orders $\rho \in [0, 1]$.

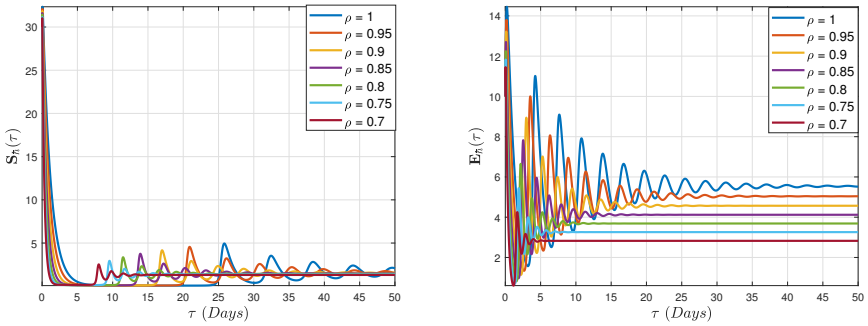

(a) **(b)**

Figure 8. Graphical illustration of the susceptible group $\mathbf{S}_{\hbar}(\tau)$ and exposed individuals $\mathbf{E}_{\hbar}(\tau)$ for the human population when $\varphi_{\hbar}$ decreases considering multiple fractional orders $\rho \in [0, 1]$.

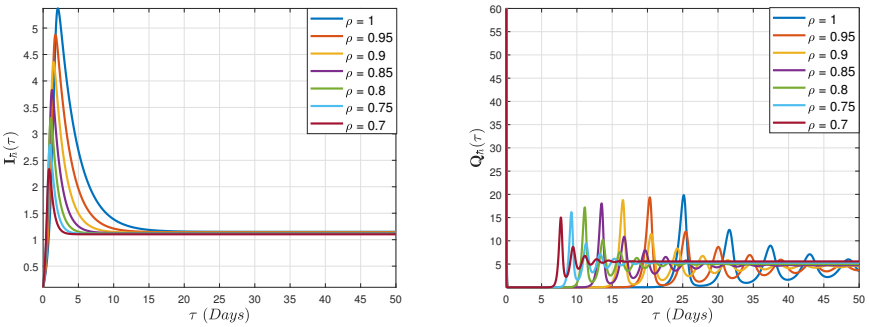

(a) **(b)**

Figure 9. Graphical illustration of the infectious group $\mathbf{I}_{\hbar}(\tau)$ and isolated individuals $\mathbf{Q}_{\hbar}(\tau)$ for the human population when $\varphi_{\hbar}$ decreases considering multiple fractional orders $\rho \in [0, 1]$.

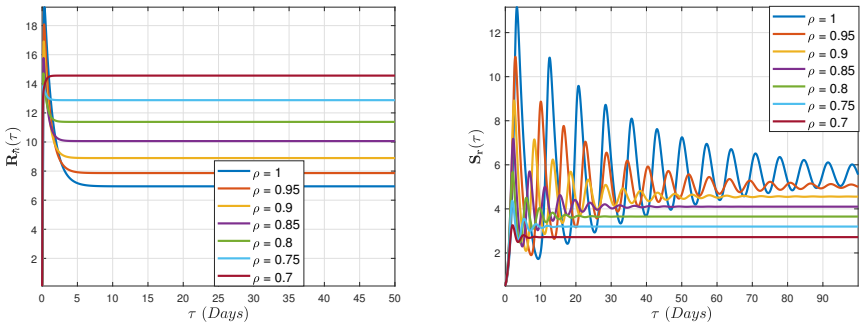

(a) **(b)**

Figure 10. Graphical illustration of the recovered human group $\mathbf{R}_{\hbar}(\tau)$ and susceptible individuals $\mathbf{S}_{\mathbf{r}}(\tau)$ for the rodent population when $\varphi_{\hbar}$ decreases considering multiple fractional orders $\rho \in [0, 1]$.

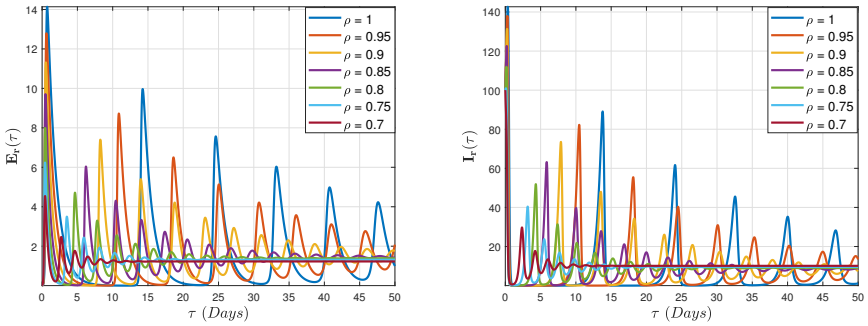

(a) **(b)**

Figure 11. Graphical illustration of the Exposed group $\mathbf{E_r}(\tau)$ and infectious individuals $\mathbf{I_r}(\tau)$ for the rodent population when $\varphi_\hbar$ decreases considering multiple fractional orders $\rho \in [0, 1]$.

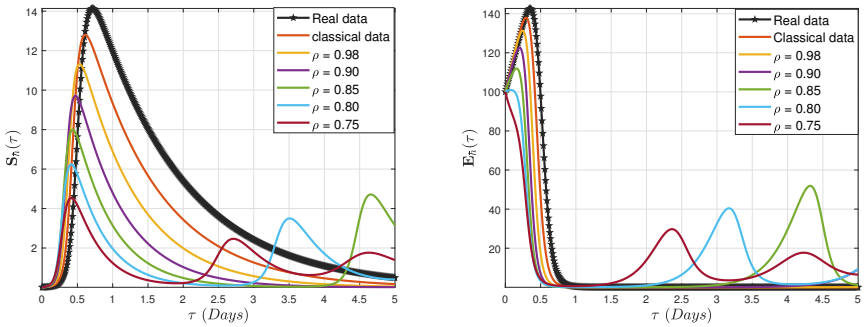

(a) **(b)**

Figure 12. Graphical illustration of the susceptible group $\mathbf{S}_\hbar(\tau)$ and exposed individuals $\mathbf{E}_\hbar(\tau)$ for the human population when ψ increases considering multiple fractional orders $\rho \in [0, 1]$.

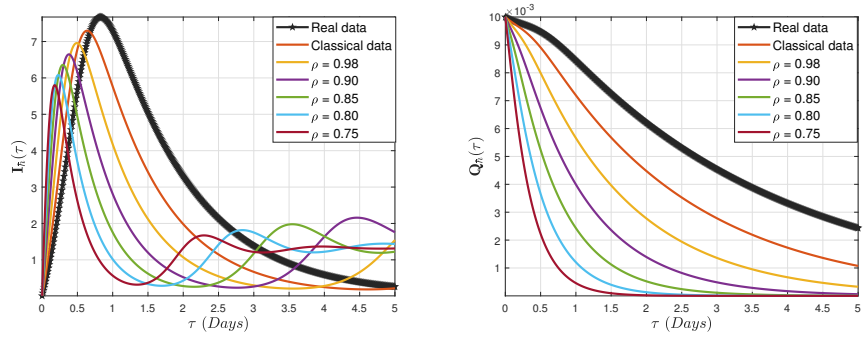

(a) **(b)**

Figure 13. Graphical illustration of the infectious group $\mathbf{I}_\hbar(\tau)$ and isolated individuals $\mathbf{Q}_\hbar(\tau)$ for the human population when ψ increases considering multiple fractional orders $\rho \in [0, 1]$.

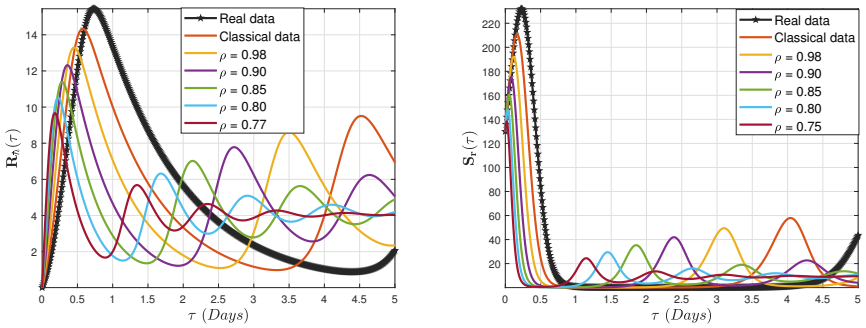

(a) **(b)**

Figure 14. Graphical illustration of the recovered human group $\mathbf{R}_{\hbar}(\tau)$ and susceptible individuals $\mathbf{S}_{\mathbf{r}}(\tau)$ for the rodent population when ψ increases considering multiple fractional orders $\rho \in [0, 1]$.

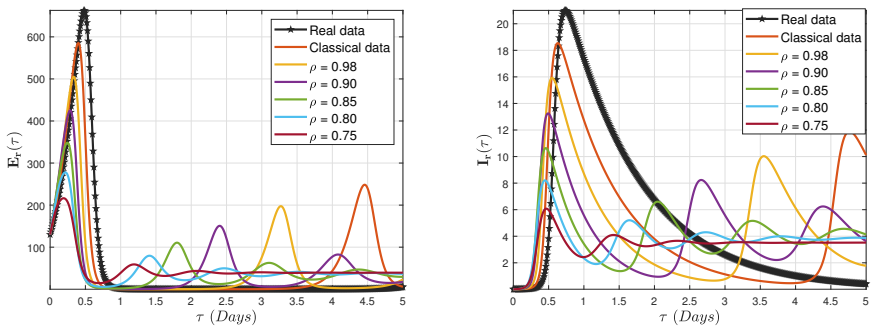

(a) **(b)**

Figure 15. Graphical illustration of the exposed group $\mathbf{E}_{\mathbf{r}}(\tau)$ and infectious individuals $\mathbf{I}_{\mathbf{r}}(\tau)$ for the rodent population when ψ increases considering multiple fractional orders $\rho \in [0, 1]$.

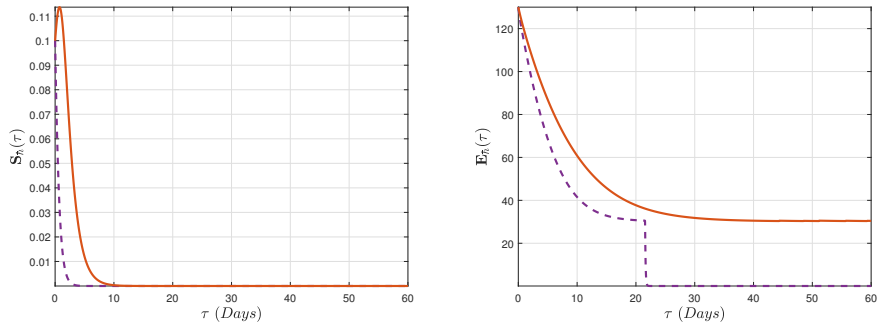

(a) **(b)**

Figure 16. Graphical illustration of the new model (3.12) for the susceptible group $\mathbf{S}_{\hbar}(\tau)$ and exposed individuals $\mathbf{E}_{\hbar}(\tau)$ for the human population without treatment (red solid line) and with treatment (blue-dotted line)

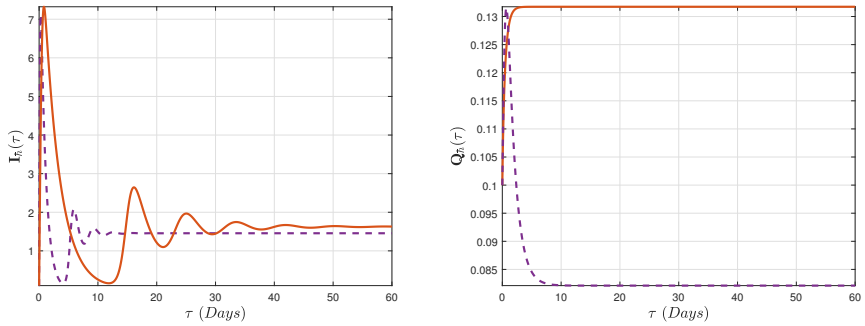

(a) **(b)**

Figure 17. Graphical illustration of the new model (3.12) for the infectious group $\mathbf{I}_{\hbar}(\tau)$ and isolated individuals $\mathbf{Q}_{\hbar}(\tau)$ for the human population without treatment (red solid line) and with treatment (blue-dotted line)

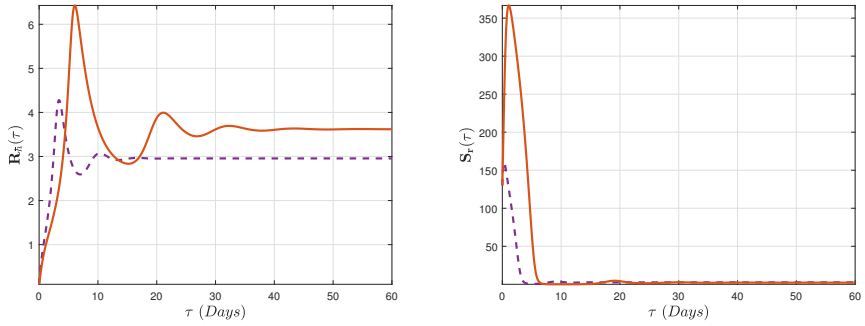

(a) **(b)**

Figure 18. Graphical illustration of the new model (3.12) for the restored human group $\mathbf{R}_{\hbar}(\tau)$ and susceptible rodent individuals $\mathbf{S}_{\mathbf{r}}(\tau)$ without treatment (red solid line) and with treatment (blue-dotted line)

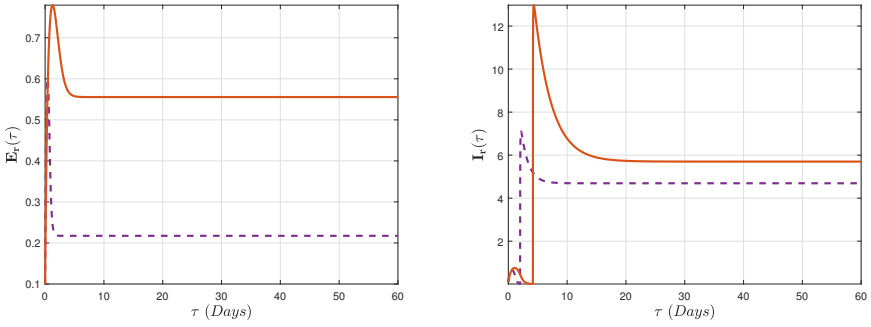

(a) **(b)**

Figure 19. Graphical illustration of the new model (3.12) for the exposed group $\mathbf{E}_{\mathbf{r}}(\tau)$ and infectious individuals $\mathbf{I}_{\mathbf{r}}(\tau)$ for the rodent population without treatment (red solid line) and with treatment (blue-dotted line)

5. Conclusions

To better comprehend the spread of $\mathbb{MPX}$ infection, a non linear deterministic mathematical model has been devised by applying the Atangana-Baleanu fractional derivative in the Caputo viewpoint. The suggested paradigm consists of eight compartments that are collectively exhaustive. The human species has been separated into five cohorts, each with its own variety of challenges. Likewise, the rodent community was classified into three categories. In addition, the essential features of the suggested framework have been demonstrated. The next-generation matrix approach was used to determine the basic reproduction value. There are two equilibria in the developed framework: a DFE point and an EEP. The stability requirements for both equilibrium conditions have been determined. Furthermore, the presence of an endemic equilibrium means that a backward bifurcation is conceivable. We have also demonstrated the interactive effects of several settings on the fractional-order by using numerical computations. According to our findings, the numerical results show that decreasing the order of the fractional derivative from 1 straightens the graphs and reduces the probability of susceptible individuals. The ABC fractional operator expressing the hereditary property is credited with this crucial breakthrough. The generalized ML function outperformed the exponential decay and index law kernels due to resilient reminiscence linked to the Atangana–Baleanu fractional derivative. Moreover, the Atangana–Baleanu fractional order derivative is also Liouville–Caputo and Caputo–Fabrizio, indicating that it has both Markovian and non-Markovian features. We, the investigators of this extensive review on the impact of various fractional formulations, including fractal–fractional derivatives, who have also analyzed the efficiency of the ABC fractional operator results on systems characterized by numerous and additional prevalent pathogen systems, may validate this notion.

Conflict of interest

The authors declare that there is no conflict of interest.

References

1. A. W. Rimoin, P. M. Mulembakani, S. C. Johnstonm, J. O. Lloyd Smith, N. K. Kisalu, T. L. Kinkela, et al., Major increase in human monkeypox incidence 30 years after smallpox vaccination campaigns cease in the Democratic Republic of Congo, *Proc. Natl. Acad. Sci. USA*, **107** (2010), 16262–16267. http://dx.doi.org/10.1073/pnas.1005769107
2. N. Sklenovská, M. Van Ranst, Emergence of monkeypox as the most important orthopoxvirus infection in humans, *Front. Public Health*, **241** (2018). https://doi.org/10.3389/fpubh.2018.00241
3. *Singapore Ministry of Health*, Europe, US on alert over detection of Monkeypox cases: What is the virus, symptoms and its transmission across the globe. Available from: https://news.knowledia.com/IN/en/articles/europe-us-on-alert-over-detection-of-monkeypox-cases-what-is-the-virus-5.
4. F. Fenner, D. A. Henderson, I. Arita, Z. Jezek, I. D. Ladnyi, Smallpox and its eradication, *W. H. O.*, 1988.

5. R. B. Kennedy, J. M. Lane, D. A. Henderson, G. A. Poland, *Smallpox and vaccinia, Vaccines (chapter 32)*, Amsterdam: Elsevier, (2012), 718–727.

6. P. E. M. Fine, Z. Jezek, B. Grab, H. Dixon, The transmission potential of monkeypox virus in human populations, *Int. J. Epidemiol.*, **17** (1988), 643–650. http://dx.doi.org/10.1093/ije/17.3.643

7. K. D. Reed, J. W. Melski, M. B. Graham, R. L. Regnery, M. J. Sotir, M. V. Wegner, et al., The detection of monkeypox in humans in the Western Hemisphere, *Engl. J. Med.*, **350** (2004), 342–350. http://dx.doi.org/10.1056/ NEJMoa032299

8. M. Roberts, Monkeypox to get a new name, says WHO. Available from: https://en.kataeb.org/articles/monkeypox-to-get-a-new-name-says-who.

9. L. A. Learned, M. G. Reynolds, D. W. Wassa, Y. Li, V. A. Olson, K. Karem, et al., Extended interhuman transmission of monkeypox in a hospital community in the Republic of the Congo, *Am. J. Trop. Med. Hygiene*, **73** (2005), 428–434. https://doi.org/10.4269/ajtmh.2005.73.428

10. R. A. Elderfield, S. J. Watson, A. Godlee, W. E. Adamson, C. I. Thompson, J. Dunning, M. Fernandez-Alonso, D. Blumenkrantz, T. Hussell, M. Zambon, Accumulation of human-adapting mutations during circulation of A (H1N1) pdm09 influenza virus in humans in the United Kingdom, *J. Virol.*, **88** (2014), 13269–13283. https://doi.org/10.1128/JVI.01636-14

11. N. C. Elde, S. J. Child, M. T. Eickbush, J. O. Kitzman, K. S. Rogers, J. Shendure, et al., Poxviruses deploy genomic accordions to adapt rapidly against host antiviral defenses, *Cell*, **150** (2012), 831–841. https://doi.org/10.1016/j.cell.2012.05.049

12. R. J. Jackson, A. J. Ramsay, C. D. Christensen, S. Beaton, D. F. Hall, I. A. Ramshaw, Expression of mouse interleukin-4 by a recombinant ectromelia virus suppresses cytolytic lymphocyte responses and overcomes genetic resistance to mousepox. *J. Virol.*, **75** (2001), 1205–1210. https://doi.org/10.1128/JVI.75.3.1205-1210.2001

13. S. Bidari, E. E. Goldwyn, Stochastic models of influenza outbreaks on a college campus, *Lett. Biomath.*, **6** (2019), 1–14. https://doi.org/10.1080/23737867.2019.1618744

14. J. C. Blackwood, L. M. Childs, An introduction to compartmental modeling for the budding infectious disease modeler. *Lett. Biomath.*, **5** (2018), 195–221. https://doi.org/10.30707/LiB5.1Blackwood

15. C. Bhunu, S. Mushayabasa, Modelling the transmission dynamics of Pox-like infections, *IAENG Int. J. Appl. Math.*, **41** (2011), 141–149.

16. S. Usman, I. I. Adamu, Modeling the transmission dynamics of the monkeypox virus infection with treatment and vaccination interventions, *J. Appl. Math. Phy.*, **5** (2017), 2335–2353. https://doi.org/10.4236/jamp.2017.512191

17. A. Atangana, D. Baleanu, New fractional derivatives with nonlocal and non-singular kernel: Theory and application to heat transfer model, *Therm. Sci.*, **20** (2016), 763–769. https://doi.org/10.2298/TSCI160111018A

18. S. A. Iqbal, M. G. Hafez, Y. M. Chu, C. Park, Dynamical Analysis of nonautonomous RLC circuit with the absence and presence of Atangana-Baleanu fractional derivative, *J. Appl. Anal. Comput.* **12** (2022), 770–789. https://doi.org/10.11948/20210324

19. Y. M. Chu, S. Bashir, M. Ramzan, M. Y. Malik, Model-based comparative study of magnetohydrodynamics unsteady hybrid nanofluid flow between two infinite parallel plates with particle shape effects, *Math. Meth. Appl. Sci.*, 2022. https://doi.org/10.1002/mma.8234

20. W. M. Qian, H. H. Chu, M. K. Wang, Y. M. Chu, Sharp inequalities for the Toader mean of order -1 in terms of other bivariate means, *J. Math. Inequal.*, **16** (2022), 127–141. https://doi.org/10.7153/jmi-2022-16-10

21. T. H. Zhao, H. H. Chu, Y. M. Chu, Optimal Lehmer mean bounds for the nth power-type Toader mean of $n = -1, 1, 3$, *J. Math. Inequal.*, **16** (2022), 157–168. https://doi.org/10.7153/jmi-2022-16-12

22. M. Caputo, M. Fabrizio, A new definition of fractional derivative without singular kernel, *Progr. Fract. Differ. Appl.*, **1** (2015), 1–13.

23. J. F. Gómez-Aguilar, H. Yéppez-Marténez, C. Calderón-Ramón, I. Cruz-Orduña, R. F. Escobar-Jiménez, V. H. Olivares-Peregrino, Modeling of a mass-spring-damper system by fractional derivatives with and without a singular kernel, *Entropy*, **17** (2015), 6289–6303. https://doi.org/10.3390/e17096289

24. F. Z. Wang, M. N. Khan, I. Ahmad, H. Ahmad, H. Abu-Zinadah, Y. M. Chu, Numerical solution of traveling waves in chemical kinetics: time-fractional fishers equations, *Fractals*, **30** (2022). https://doi.org/10.1142/S0218348X22400515

25. S. Rashid, E. I. Abouelmagd, S. Sultana, Y. M. Chu, New developments in weighted n-fold type inequalities via discrete generalized $\hat{\text{h}}$-proportional fractional operators, *Fractals*, **30** (2022). https://doi.org/10.1142/S0218348X22400564

26. S. Rashid, B. Kanwal, A. G. Ahmad, E. Bonyah, S. K. Elagan, Novel numerical estimates of the pneumonia and meningitis epidemic model via the nonsingular kernel with optimal analysis, *Complexity*, **2022** (2022), 1–25. https://doi.org/10.1155/2022/4717663

27. S. W. Yao, S. Rashid, M. Inc, E. Elattar, On fuzzy numerical model dealing with the control of glucose in insulin therapies for diabetes via nonsingular kernel in the fuzzy sense, *AIMS Math.*, **7** (2022). https://doi.org/10.3934/math.2022987

28. S. Rashid, F. Jarad, A. K. Alsharidi, Numerical investigation of fractional-order cholera epidemic model with transmission dynamics via fractal-fractional operator technique, *Chaos Solitons Fractals*, **162** (2022), 112477. https://doi.org/10.1016/j.chaos.2022.112477

29. F. Jin, Z. S. Qian, Y. M. Chu, M. ur Rahman, On nonlinear evolution model for drinking behavior under Caputo-Fabrizio derivative, *J. Appl. Anal. Comput.* **12** (2022), 790–806. https://doi.org/10.11948/20210357

30. S. Rashid, M. K. Iqbal, A. M. Alshehri, F. Jarad, R. Ashraf, A comprehensive analysis of the stochastic fractal-fractional tuberculosis model via Mittag-Leffler kernel and white noise, *Results Phy.*. **39** (2022), 105764. https://doi.org/10.1016/j.rinp.2022.105764

31. M. Al-Qurashi, S. Rashid, F. Jarad, A computational study of a stochastic fractal-fractional hepatitis B virus infection incorporating delayed immune reactions via the exponential decay, *Math. Biosci. Eng*, **19** (2022), 12950–12980. https://doi.org/10.3934/mbe.2022605

32. S. Rashid, A. Khalid, S. Sultana, F. Jarad, K. M. Abulanja, Y. S. Hamed, Novel numerical investigation of the fractional oncolytic effectiveness model with M1 virus via generalized fractional derivative with optimal criterion, *Results Phy.*, **37** (2022), 105553. https://doi.org/10.1016/j.rinp.2022.105553
33. S. Rashid, B. Kanwal, F. Jarad, S. K. Elagan, A peculiar application of the fractal-fractional derivative in the dynamics of a nonlinear scabies model, *Results Phys.*, **38** (2022), 105634. https://doi.org/10.1016/j.rinp.2022.105634
34. S. Rashid, Y. G. Sánchez, J. Singh, Kh. M. Abualnaja, Novel analysis of nonlinear dynamics of a fractional model for tuberculosis disease via the generalized Caputo fractional derivative operator (case study of Nigeria), *AIMS Math.*, **7** (2022), 10096–10121. https://doi.org/10.3934/math.2022562
35. S. Rashid, F. Jarad, A. G. Ahmad, Kh. M .Abualnaja, New numerical dynamics of the heroin epidemic model using a fractional derivative with Mittag-Leffler kernel and consequences for control mechanisms, *Results Phys.*, **35** (2022), 105304. https://doi.org/10.1016/j.rinp.2022.105304
36. S. N. Hajiseyedazizi, M. E. Samei, J. Alzabut, Y. M. Chu, On multi-step methods for singular fractional q-integro-differential equations, *Open Math.* **19** (2021), 1378–1405. https://doi.org/10.1515/math-2021-0093
37. S. Rashid, E. I. Abouelmagd, A. Khalid, F. B. Farooq, Y. M. Chu, Some recent developments on dynamical $\hbar$-discrete fractional type inequalities in the frame of nonsingular and nonlocal kernels, *Fractals*, **30** (2022). https://doi.org/10.1142/S0218348X22401107
38. Y. M. Chu, U. Nazir, M. Sohail, M. M. Selim, J. R. Lee, Enhancement in thermal energy and solute particles using hybrid nanoparticles by engaging activation energy and chemical reaction over a parabolic surface via finite element approach, *Fractal Fract.* **5** (2021), 119. https://doi.org/10.3390/fractalfract5030119
39. T. Abdeljawad, D. Baleanu, Integration by parts and its applications of a new nonlocal fractional derivative with Mittag-Leffler nonsingular kernel, *J. Nonlinear Sci. Appl.*, **10** (2017), 1098–1107. http://dx.doi.org/10.22436/jnsa.010.03.20
40. J. Singh, D. Kumar, D. Baleanu, On the analysis of fractional diabetes model with exponential law, *Adv. Differ. Equ.*, **2018** (2018), 231. https://doi.org/10.1186/s13662-018-1680-1
41. Z. M. Odibat, N. T. Shawagfeh, Generalized Taylor's formula, *Appl. Math. Comput.* **186** (2007), 286–293. https://doi.org/10.1016/j.amc.2006.07.102
42. S. V. Bankuru, S. Kossol, W. Hou, P. Mahmoudi, J. Rychtáî, D. Taylor, A game-theoretic model of Monkeypox to assess vaccination strategies, *PeerJ*, **8** (2020), 9272. http://doi.org/10.7717/peerj.927
43. O. J. Peter, S. Kumar, N. Kumari, F. A. Oguntolu, K. Oshinubi, R. Musa, Transmission dynamics of Monkeypox virus: A mathematical modelling approach, *Model. Earth Sys. Envir.*, 2021. https://doi.org/10.1007/s40808-021-01313-2
44. M. Toufik, A. Atangana, New numerical approximation of fractional derivative with non-local and non-singular kernel: Application to chaotic models, *Eur. Phys. J. Plus*, **132** (2017), 444. https://doi.org/10.1140/epjp/i2017-11717-0

45. C. Bhunu, W. Garira, G. Magombedze, Mathematical analysis of a two strain hiv/aids model with antiretroviral treatment. *Acta Biotheor.*, **57** (2009), 361–381. https://doi.org/10.1007/s10441-009-9080-2

46. C. Bhunu, S. Mushayabasa, Modelling the transmission dynamics of pox-like infections, *IAENG Int. J. Appl. Math.*, **41** (2011), 141–149.

47. M. R. Odom, R. Curtis Hendrickson, E. J. Lefkowitz, Poxvirus protein evolution: Family wide assessment of possible horizontal gene transfer events, *Virus Res.*, **144** (2009), 233–249. https://doi.org/10.1016/j.virusres.2009.05.006

48. Y. Lia, Y. Chen, I. Podlubny, Mittag–Leffler stability of fractional order nonlinear dynamic systems, *Automatica*, **45** (2009), 1965–1969. https://doi.org/10.1016/j.automatica.2009.04.003

49. S. Somma, N. Akinwande, U. Chado, A mathematical model of monkey pox virus transmission dynamics, *IFE J. Sci.*, **21** (2019), 195–204. https://doi.org/10.4314/ijs.v21i1.17

50. O. Diekmann, J. Heesterbeek, M. G. Roberts, The construction of next-generation matrices for compartmental epidemic models, *J. R. Soc. Interface*, **7** (2010), 873–885. https://doi.org/10.1098/rsif.2009.0386

51. P. van den Driessche, J. Watmough, *Further notes on the basic reproduction number*, Springer, Berlin, Heidelberg, (2008), 159–178.

52. C. Castillo-Chavez, B. Song, Dynamical models of tuberculosis and their applications, *Math. Biosci. Eng.*, **1** (2004), 361. https://doi.org/10.3934/mbe.2004.1.361

53. E. Ahmed, A. M. A. El-Sayed, H. A. A. El-Saka, On some routh–hurwitz conditions for fractional order differential equations and their applications in lorenz, rössler, chua and chen systems, *Phys. Lett. A*, **358** (2006), 1–4. https://doi.org/10.1016/j.physleta.2006.04.087

54. C. T. Deressa, G. F. Duressa, Analysis of Atangana–Baleanu fractional-order SEAIR epidemic model with optimal control, *Adv. Diff. Equ.*, **2021** (2021), 174. https://doi.org/10.1186/s13662-021-03334-8

55. B. Wu, F. Fu, L. Wang, Imperfect vaccine aggravates the long-standing dilemma of voluntary vaccination, *PLOS ONE*, **6** (2011), 20577. https://doi.org/10.1371/journal.pone.0020577

56. L. Khodakevich, Z. Ježek, D. Messinger, Monkeypox virus: Ecology and public health significance, *Bull. W. H. O.*, **66** (1988), 747–752.

57. J. Kobe, N. Pritchard, Z. Short, I. V. Erovenko, J. Rychtář, J. T. Rowel, A game theoretic model of cholera with optimal personal protection strategies. *Bull. Math. Bio.*, **80** (2018), 2580–2599. https://doi.org/10.1007/s11538-018-0476-5

AIMS Press